2 Results of Superconducting Accelerator Development

2.1 Superconducting Cavities

2.1.1 Introduction

Historically, the main drawback of superconducting (sc) accelerating structures has been the low gradient of the cavities combined with the high cost of cryogenic equipment. At the time of the first TESLA workshop [1] superconducting RF cavities in particle accelerators were usually operated in the 5 MV/m regime; such low gradients would make a superconducting linear electron-positron collider non-competitive with normal-conducting colliders, and hence the ambitious design gradient of 25 MV/m was specified for TESLA. As of writing, this gradient has been exceeded in multicell niobium cavities produced by industry. In addition, the cost per unit length of the linac has been considerably reduced by applying economical cavity production methods and by assembling many cavities in a long cryostat.

The TESLA cavities are similar in layout to the 5-cell 1.5 GHz cavities of the electron accelerator CEBAF, which were developed at Cornell University and fabricated by industry [2]. At that time the cavities considerably exceeded the design gradient of 5 MV/m: hence they were considered to have a significant potential for further improvement, and the CEBAF cavity manufacturing methods were adopted for TESLA. Improved quality control of the superconducting material and of the fabrication methods were made, and important new steps were introduced into the cavity preparation:

- chemical removal of a thicker layer from the inner cavity surface;
- a 1400°C annealing with a titanium getter to improve the niobium heat conductivity and to homogenise the material;
- rinsing with ultra-pure water at high pressure (100 bar) to remove surface contaminants;
- destruction of field emitters using High Power Processing.

Application of the above techniques — combined with an extremely careful handling of the cavities in a clean-room environment — has led to accelerating fields which exceed the original TESLA-500 design goal of 25 MV/m.

The TESLA Test Facility (TTF) has been set up at DESY to provide the infrastructure for the chemical treatment, clean-room assembly, and testing of industrially

produced multicell cavities. An electron linac has been built as a test bed for the performance of the sc accelerating structures with an electron beam of high bunch charge. The linac is also equipped with undulator magnets to generate FEL radiation in the VUV regime.

2.1.2 Superconducting material

2.1.2.1 Choice of superconductor

The existing large scale applications for superconductors are magnets and accelerating cavities. A common requirement is a high critical temperature[1], but there are distinct differences concerning the critical magnetic field. In magnets operated with a dc or a low-frequency ac current, 'hard' (type I) superconductors are required, with high upper critical fields (15–20 T) and strong flux pinning in order to achieve high current density; such properties are only offered by alloys like niobium-titanium or niobium-tin. In microwave applications the limit is essentially set by the thermodynamic critical field, which is well below 1 T for all known superconductors. Strong flux pinning is undesirable as it is coupled with losses due to hysteresis. Hence a 'soft' (type II) superconductor must be used. Pure niobium is the best candidate, although its critical temperature T_c is only 9.2 K, and the thermodynamic critical field about 200 mT. Niobium-tin (Nb_3Sn) with a critical temperature of 18 K looks more favourable at first sight, however the gradients achieved in Nb_3Sn coated niobium cavities were always below 15 MV/m, probably due to grain boundary effects in the Nb_3Sn layer [3]. For this reason the TESLA collaboration decided to use niobium as the superconducting material. Among the two options — cavities made from solid niobium or by sputter-coating of a copper cavity — the solid niobium approach promised higher accelerating gradients and was adopted as the baseline for the TESLA cavity R&D program.

2.1.2.2 Microwave surface resistance

Superconductors suffer from energy dissipation in microwave fields since the radio frequency (RF) magnetic field penetrates a thin surface layer and induces oscillations of the unpaired electrons. According to the Bardeen-Cooper-Schrieffer (BCS) theory of superconductivity, the surface resistance is given by the expression

$$R_{\mathrm{BCS}} \propto \frac{f^2}{T} \exp(-1.76\, T_c/T),$$

where f is the microwave frequency. For niobium the BCS surface resistance at 1.3 GHz is about 800 nΩ at 4.2 K, and drops to 15 nΩ at 2 K (see figure 2.1.1). Because of the exponential temperature dependence, operation at 1.8–2 K is essential for achieving high accelerating gradients in combination with very high quality (Q) factors. Superfluid helium is an excellent coolant owing to its high heat conductivity. In addition to the

[1] The High-T_c ceramic superconductors have not yet found widespread application in magnets, mainly due to technical difficulties in cable production and coil winding. Cavities with High-T_c sputter coatings on copper have shown much inferior performance in comparison to niobium cavities.

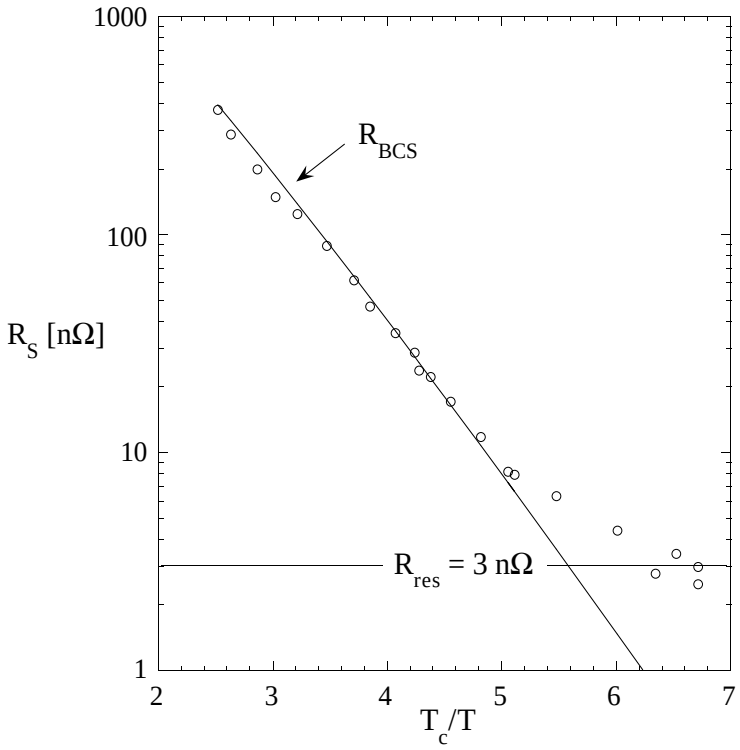

Figure 2.1.1: *The measured surface resistance of a 9-cell TESLA cavity plotted as a function of T_c/T. The residual resistance of 3 nΩ corresponds to a quality factor $Q_0 = 10^{11}$.*

BCS term there is a residual resistance R_{res} caused by impurities, frozen-in magnetic flux, or lattice distortions. This term is temperature independent and amounts to a few nΩ for very pure niobium, but increases dramatically if the surface is contaminated.

2.1.2.3 Heat conduction in niobium

The heat produced at the inner cavity surface has to be guided through the cavity wall to the superfluid helium bath. The thermal conductivity of niobium exhibits a strong temperature dependence in the cryogenic regime (see figure 2.1.2) and scales approximately with the residual resistivity ratio[1] *RRR*.

Impurities have a strong impact on the thermal conductivity, and niobium with contamination in the ppm range is required. At the niobium-helium interface a temperature jump is observed due to the so-called Kapitza resistance: for a clean niobium surface in contact with superfluid helium at 2 K, the effect gives a temperature rise per unit power flux of about $1.6 \cdot 10^{-4}\,\text{K}/(\text{Wm}^{-2})$ [4].

[1] *RRR* is defined as the ratio of the resistivities at room temperature and at liquid helium temperature. The low temperature resistivity is usually measured at 4.2 K, applying a magnetic field to assure the normal state.

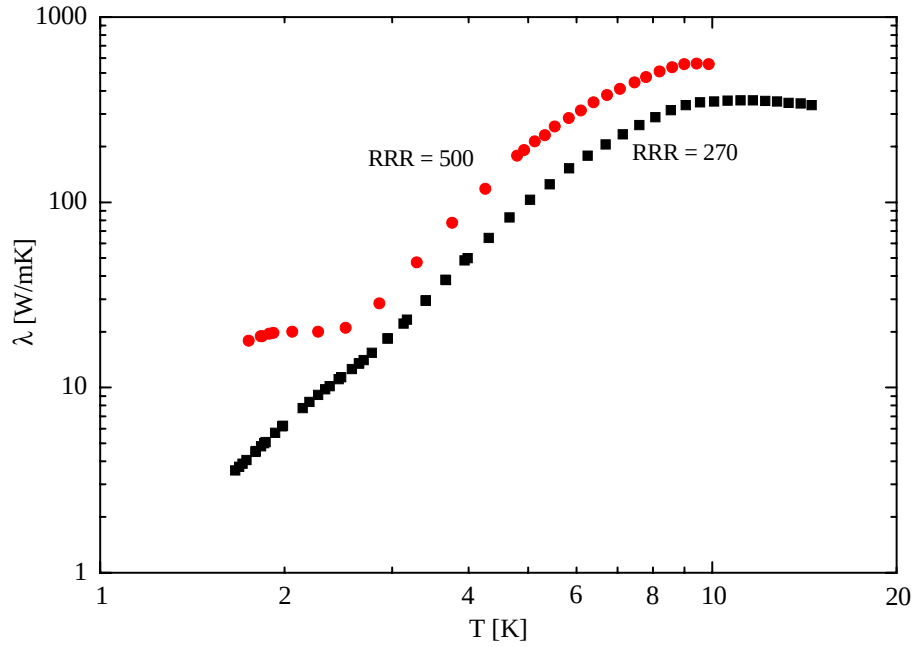

Figure 2.1.2: *Measured heat conductivity of samples from the niobium sheets used in the TESLA cavities: before and after the 1400° C heat treatment ($RRR = 280$ and $RRR = 500$ respectively).*

2.1.2.4 Magnetic field effects

Maximum gradient. Superconductivity breaks down when the microwave magnetic field at the cavity surface exceeds a critical value. The limit is close to the thermodynamic critical field B_c (200 mT for niobium at 2 K). The corresponding accelerating field on the cavity axis is about 50 MV/m for the TESLA cavity geometry. Several authors claim that RF superconductivity persists up to a so-called 'superheating field', exceeding B_c by 20% in case of Nb: however it remains to be proven that RF cavities can be reliably operated near or even beyond B_c.

Trapped magnetic flux. Although niobium is a soft type II superconductor without strong flux pinning, weak magnetic dc fields are not expelled upon cool-down but remain trapped in the niobium. Each flux line contains a normal-conducting core. Trapped magnetic flux contributes to the surface resistance by an amount of $3.5\,\mathrm{n}\Omega/\mu\mathrm{T}$ for niobium. Therefore, to achieve $Q_0 \geq 10^9$ the TESLA cavities are magnetically shielded.

2.1.3 Design of the TESLA cavities

The TESLA cavity is a 9-cell standing wave structure of about 1 m length whose fundamental TM mode has a frequency of 1300 MHz. The cavity is made from solid niobium and is bath-cooled by superfluid helium at 2 K. Each cavity is equipped with:

a helium tank; a tuning system driven by a stepping motor; a coaxial RF power coupler; a pickup probe; and two higher-order mode (HOM) couplers.

2.1.3.1 Choice of frequency and cavity geometry

Cost economy in a long linac calls for a small cavity design and consequently a frequency well above the 350 to 500 MHz used in storage rings like LEP or HERA. The frequency can not be made arbitrarily high, however, because of the f^2 dependence of the BCS surface resistance, which at 3 GHz already limits the attainable gradient to about 30 MV/m [5]. Another reason to stay below 3 GHz is the wakefields which scale with the second to third power of the frequency ($W_\parallel \propto f^2$, $W_\perp \propto f^3$). The optimum frequency is in the 1.5 GHz regime; the choice for 1.3 GHz was motivated by the availability of high power klystrons.

A multicell structure is needed to maximise the active acceleration length in a linac. An upper limit on the number of cells per cavity is given by the requirements of field homogeneity throughout the structure and the absence of trapped modes (see below). A 9-cell structure is close to the optimum. A side view of the TTF cavity with the beam tube sections and the coupler ports is shown in figure 2.1.3.

The cells have a spherical contour near the equator for low multipacting sensitivity, and a large iris radius to reduce wakefield effects. The resonator is operated in the π-mode with 180° phase difference between adjacent cells. The cell length is determined by the condition that the electric field has to be inverted in the time a relativistic particle needs to travel from one cell to the next. The end cells have a slightly different shape to ensure equal field amplitudes in all 9 cells. In addition there is a small asymmetry between the left and right end cell which reduces trapping of higher-order modes. The important cavity parameters are listed in table 2.1.1.

2.1.3.2 Lorentz-force detuning and cavity stiffening

The RF electromagnetic field exerts Lorentz forces on the currents induced in a thin surface layer, resulting in a deformation of the cells in the μm range. The computed frequency shift at 25 MV/m is 900 Hz for an unstiffened cavity of 2.5 mm wall thickness. The bandwidth of the cavity equipped with the main power coupler ($Q_{ext} = 2.5 \cdot 10^6$) is about 520 Hz (FWHM): hence a reinforcement of the cavity is needed to reduce the detuning. Niobium stiffening rings are welded in between adjacent cells as shown in figure 2.1.4. They reduce the frequency shift by a factor of two[1].

2.1.4 Cavity fabrication and treatment

The superconducting resonators are fabricated from bulk niobium by electron-beam (EB) welding of deep-drawn half cells. The tubes for the beam pipes and the coupler ports are made by back extrusion and are joined to the cavity by EB welds.

[1] Part of the remaining shift is due to an elastic deformation of the tuning mechanism.

type of accelerating structure	standing wave
accelerating mode	TM_{010} , π-mode
fundamental frequency	1300 MHz
nominal gradient E_{acc} for TESLA-500	23.4 MV/m
quality factor Q_0	$> 10^{10}$
active length L	1.038 m
cell-to-cell coupling k_{cc}	1.87 %
iris diameter	70 mm
R/Q	1036 Ω
E_{peak}/E_{acc}	2.0
B_{peak}/E_{acc}	4.26 mT/(MV/m)
tuning range	± 300 kHz
$\Delta f/\Delta L$	315 kHz/mm
Lorentz force detuning constant K_{Lor}	$\approx 1\,\mathrm{Hz/(MV/m)^2}$
Q_{ext} of input coupler	$2.5{\cdot}10^6$
cavity bandwidth at $Q_{ext} = 2.5 \cdot 10^6$	520 Hz FWHM
fill time	420 μs
number of HOM couplers	2

Table 2.1.1: *Parameters of the 9-cell cavity (note that we adopt here the definition of shunt impedance by the relation $R = V^2/P$, where P is the dissipated power and V the peak voltage in the equivalent parallel LCR circuit).*

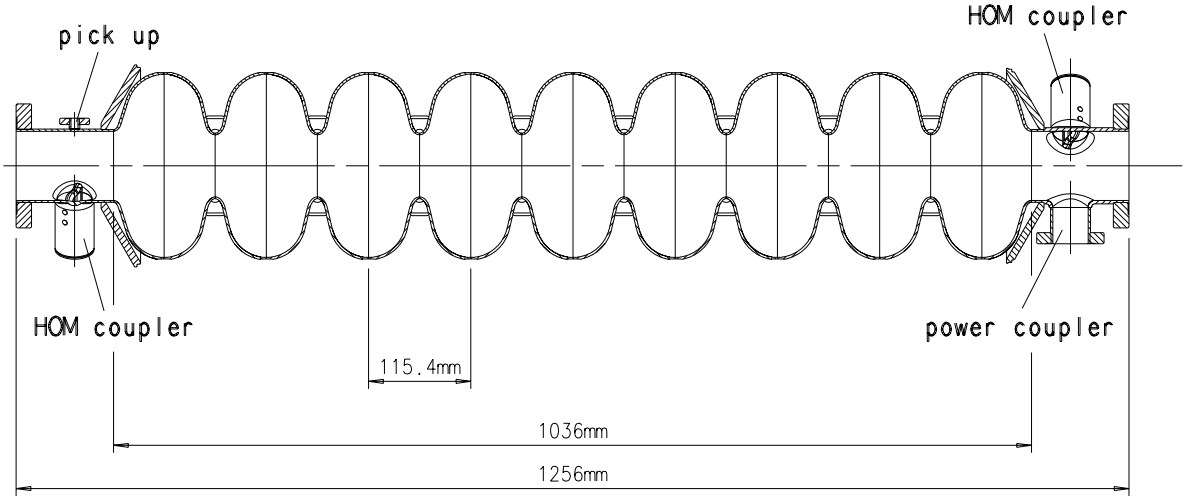

Figure 2.1.3: *Side view of the 9-cell cavity with the main power coupler port and two higher-order mode couplers.*

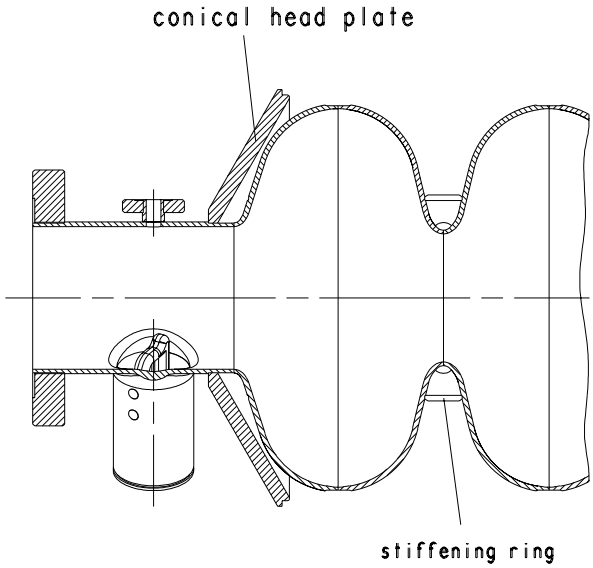

Figure 2.1.4: *End section of a cavity with stiffening ring and conical head plate for welding into the helium tank.*

Impurity content in ppm (wt)				Mechanical Properties	
Ta	≤ 500	H	≤ 2	Residual resistivity ratio RRR	≥ 300
W	≤ 70	N	≤ 10	grain size	$\approx 50\ \mu$m
Ti	≤ 50	O	≤ 10	yield strength	> 50 MPa
Fe	≤ 30	C	≤ 10	tensile strength	> 100 MPa
Mo	≤ 50			elongation at break	30 %
Ni	≤ 30			Vickers hardness HV 10	≤ 50

Table 2.1.2: *Technical specification for niobium used in TESLA cavities.*

2.1.4.1 Niobium specification

The niobium specification for the TESLA cavities is listed in table 2.1.2. The most important metallic impurity in niobium is tantalum, with a typical concentration of 500 ppm. The interstitially dissolved gases (mainly oxygen) act as scattering centres for the unpaired electrons and reduce the thermal conductivity. The niobium ingot is out-gassed by several melting cycles in a high vacuum electron beam furnace. The interstitial oxygen, nitrogen and carbon contamination is reduced to a few ppm.

The Nb ingots are forged and rolled into sheets of 2.8 mm thickness. After rolling the Nb sheets are first degreased and cleaned by chemical etching. The sheets are then annealed for 1–2 hours at 700–800° C in a vacuum oven at 10^{-5}–10^{-6} mbar to achieve full recrystallization and a uniform grain size of about 50 μm. The finished Nb sheets are eddy-current checked for defects like cracks or foreign inclusions which might impair the superconducting properties.

2.1.4.2 Cavity fabrication

Cavity fabrication is a delicate procedure, requiring intermediate cleaning steps and a careful choice of the weld parameters to achieve full penetration of the joints. First, two half cells are connected at the iris; the stiffening rings are welded in next. At this point weld shrinkage may lead to a slight distortion of the cell shape which needs to be corrected. Particularly critical are the equator welds which are made from the outside, and a reliable method for obtaining a smooth weld seam at the *inner* cavity surface was required. A two-pass procedure was developed, where 50% of the power is applied to the first weld pass, and 100% on the second. In both cases, a slightly defocused electron beam rastered in an elliptic pattern is used. The electron-beam welding technique of niobium cavities has been perfected in industry to such an extent that the weld seams do not limit cavity performance below ∼30 MV/m.

A challenge for a welded construction are the tight mechanical and electrical tolerances. These can be maintained by a combination of mechanical and radio frequency measurements on half cells and by careful tracking of weld shrinkage. The procedures established during the TTF cavity fabrication are suitable for large series production, requiring quality assurance measurements only on a small sample of cavities.

The cavities are equipped with niobium-titanium flanges at the beam pipes and the coupler ports[1]. NbTi can be electron-beam welded to niobium and possesses a surface hardness equivalent to that of standard UHV flange material (stainless steel 316 LN/ DIN 1.4429). Contrary to pure niobium, the alloy NbTi (ratio 45/55 by weight) shows no softening after the heat treatment at 1400°C and only a moderate crystal growth. O-ring type aluminum gaskets provide reliable seals in superfluid helium.

2.1.4.3 Cavity treatment

A layer of 100–200 μm is removed in several steps from the inner cavity surface to obtain good RF performance in the superconducting state. The standard method applied at DESY is called Buffered Chemical Polishing (BCP) [6], and uses an acid mixture of HF (48 %), HNO_3 (65 %) and H_3PO_4 (85 %) in the ratio 1:1:2. The acid is cooled to 5°C and pumped through the cavity in a closed loop. After rinsing with ultra-pure water and drying in a class 100 clean room, the cavities are annealed at 800°C in an Ultra High Vacuum (UHV) oven to out-gas dissolved hydrogen and relieve mechanical stress in the deep drawn niobium. In a second UHV oven the cavities are heated to 1350–1400°C at which temperature the other dissolved gases diffuse out of the material, and the residual resistivity ratio *RRR* increases by about a factor of two to around 500. To absorb the oxygen diffusing out of the niobium and to prevent oxidation by the residual gas in the oven (pressure $< 10^{-7}$ mbar), a thin titanium layer is evaporated on the inner and outer cavity surface (Ti being a stronger getter than Nb). The titanium layer is later removed by 80 μm and 20 μm BCP of the inner and outer cavity surface respectively. This high-temperature treatment with Ti getter is referred to as post-purification. A severe drawback of post-purification is the considerable grain growth

[1] Except the first production series.

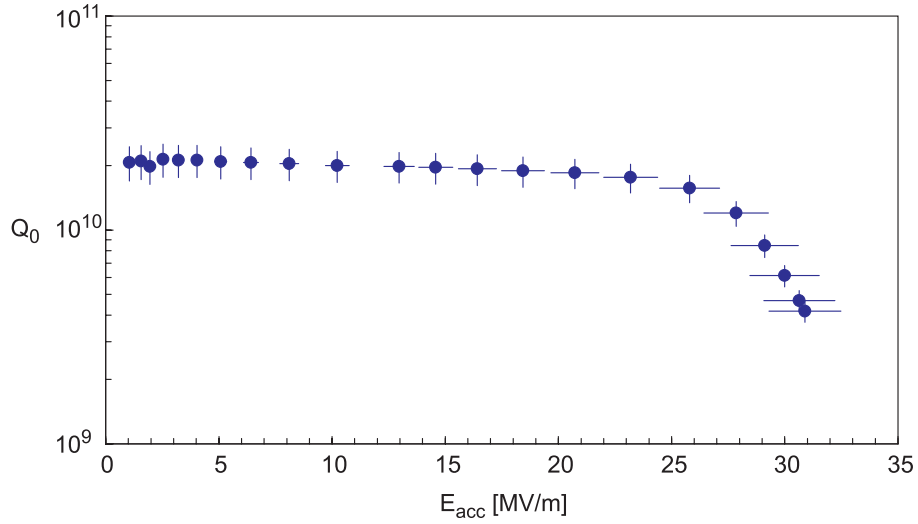

Figure 2.1.5: *Excitation curve of a high-performance 9-cell cavity. The cavity was cooled by superfluid helium of 2 K. The systematic rms errors in the determination of the accelerating field and the quality factor are indicated.*

of the niobium: post-purified cavities are vulnerable to plastic deformation and have to be handled with great care.

After the final heat treatment, the cavities are mechanically tuned to adjust the resonance frequency to the design value and to obtain equal field amplitudes in all 9 cells. This is followed by a light BCP, three steps of high-pressure water rinsing (100 bar), and drying in a class 10 clean room. The final acceptance step is an RF test in a superfluid helium bath cryostat.

2.1.5 Cavity performance and quality control measures

2.1.5.1 Practical limitations of superconducting cavities

Figure 2.1.5 shows the 'excitation curve' of a high-performance 9-cell resonator; plotted is the quality factor Q_0 as a function of the accelerating electric field E_{acc}. An almost constant high value of more than 10^{10} is observed up to 25 MV/m. The drop of Q_0 at higher gradients indicates that even the best multicell cavities are still far from reaching the theoretical limit of about 50 MV/m: the performance is limited because the superconducting surface is not perfect.

The fundamental advantage of superconducting cavities is their extremely low surface resistance at 2 K leading to RF losses which are 5 to 6 orders of magnitude lower than in copper cavities. The drawback is that even tiny surface contaminations are potentially harmful as they decrease the quality factor and may even lead to a thermal breakdown (quench) of the superconductor due to local over-heating. Perfect cleaning of the inner cavity surface is of utmost importance. Cavity treatment and assembly is therefore carried out in clean rooms conforming to semiconductor standards.

Two frequently encountered effects which degrade performance are field emission of electrons and multipacting. Field emission of electrons from sharp tips has been a notorious limitation of high-gradient superconducting cavities. In field-emission loaded cavities the quality factor drops exponentially above a certain threshold field and X-rays are observed. There is ample evidence that small particles or dust on the cavity surface act as field emitters. High quality cleaning (e.g. by rinsing with high-pressure ultra-pure water) is the most effective remedy [7]. Using high-pressure rinsing it has been possible to raise the threshold for field emission in multicell cavities from about 10 MV/m to more than 20 MV/m in the past few years. Remaining emitters can often be destroyed by 'conditioning' the cavity with short RF pulses of high instantaneous power [8] (up to 500 kW for a 1 m long TESLA cavity).

2.1.5.2 Results from the first series of TTF cavities

The first series of 27 nine-cell resonators, fully equipped with flanges for the main power and higher-order mode couplers, were produced by four European companies during the years 1994/95. These cavities were foreseen for installation in the TTF linac with a gradient of at least 15 MV/m at $Q_0 > 3 \cdot 10^9$. In the specification given to the companies, however, no guaranteed gradient was required. According to the test results at TTF these resonators fall into four classes:

(1) 16 cavities without any known material and fabrication defects, or with minor defects which could be repaired;

(2) 3 cavities with serious material defects;

(3) 6 cavities with imperfect equator welds;

(4) 2 cavities with serious fabrication defects (not fully penetrated electron beam welds or with holes burnt during welding; these were rejected).

The test results for the cavities of class 1 in a vertical bath cryostat with superfluid helium cooling at 2 K are summarized in figure 2.1.6. With the exception of two cavities, the TTF design goal of 15 MV/m is exceeded. Nine of the resonators achieve the more demanding TESLA specifications of $E_{acc} \geq 23.4$ MV/m at $Q_0 \geq 1 \cdot 10^{10}$.

The excitation curves of the class 2 cavities (figure 2.1.7) are characterized by sudden drops in quality factor with increasing field, and rather low maximum gradients. Temperature mapping revealed excessive heating at isolated spots; an example is shown in figure 2.1.8a. An eddy-current scan, performed at the Bundesanstalt für Materialforschung in Berlin (BAM), showed a pronounced signal at the defect location. With X-ray radiography (also carried out at BAM) a dark spot with a size of 0.2–0.3 mm was seen (figure 2.1.8b), indicating an inclusion of foreign material with a higher nuclear charge than niobium. Using X-ray fluorescence at HASYLAB the inclusion was identified as tantalum.

The six cavities in class 3 were all produced by one company and exhibited premature quenches at gradients of 10–14 MV/m, and a slope in the excitation curve $Q(E)$

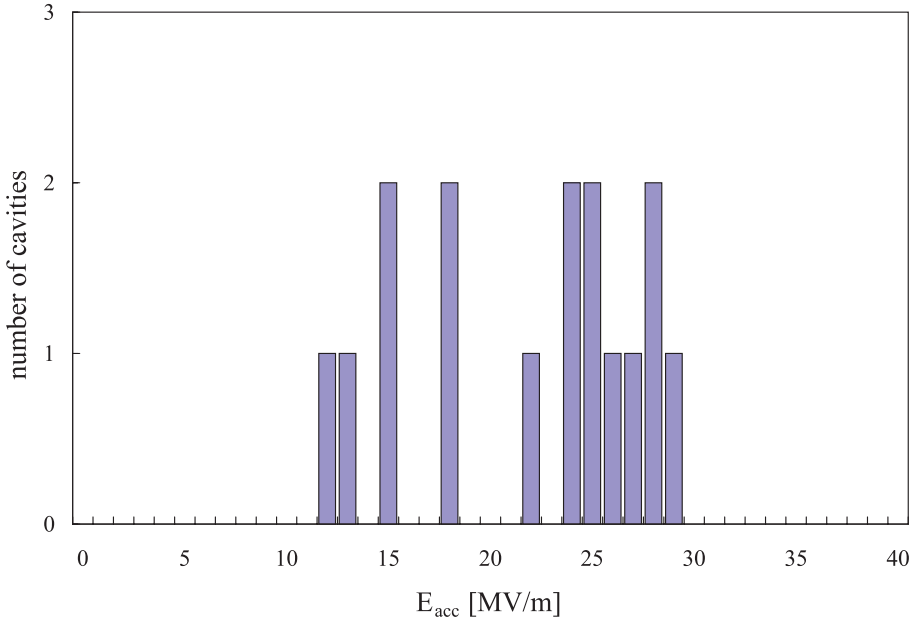

Figure 2.1.6: *Distribution of maximum gradients for the resonators of class 1, requiring a quality factor* $Q_0 \geq 1 \cdot 10^{10}$.

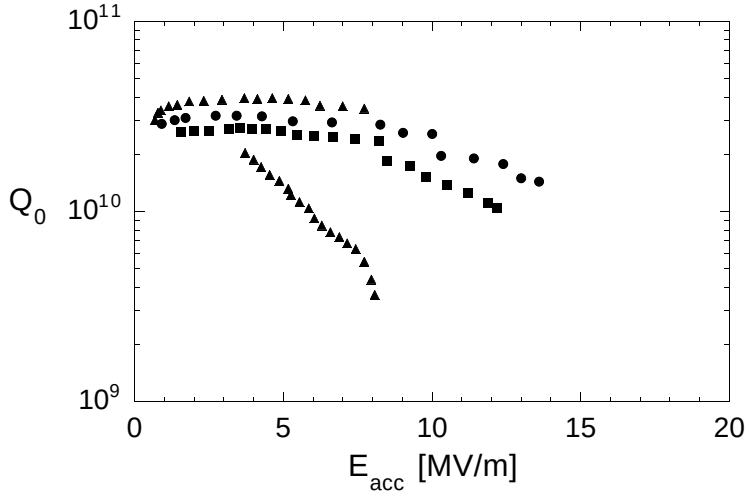

Figure 2.1.7: *Excitation curves of the three cavities with serious material defects (class 2). Cavity C5 (▲) exhibited a jump in quality factor.*

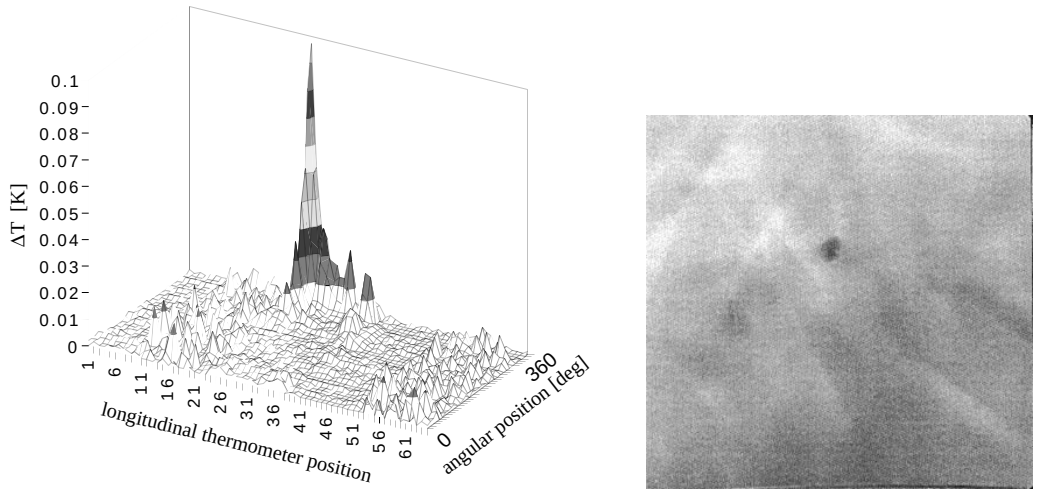

(a) (b)

Figure 2.1.8: *(a) Temperature map of cell 5 of cavity C6 showing excessive heating at a localized spot. (b) Positive print of an X-ray radiograph showing the 'hot spot' as a dark point.*

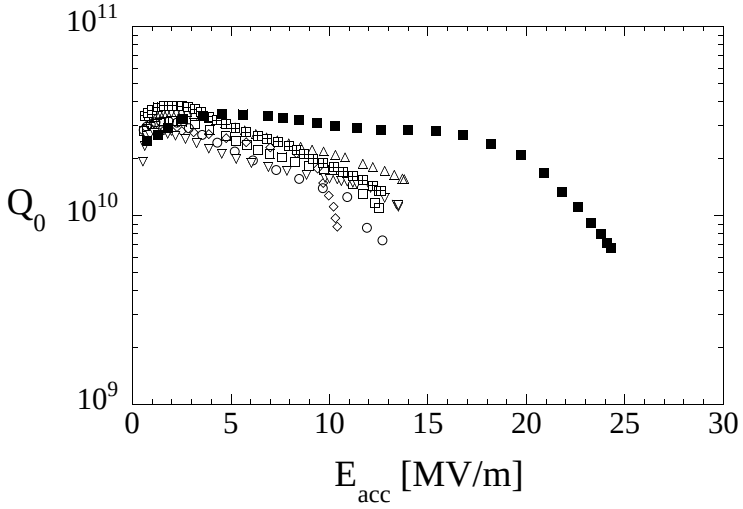

Figure 2.1.9: *Excitation curves of the six cavities with imperfect equator welds (class 3). Also shown is a resonator (■) made later by the same company, observing stringent cleaning procedures at the equator welds.*

(figure 2.1.9). Temperature mapping revealed strong heating at several spots on the equator weld and pointed to contamination of the weld seam. A new resonator manufactured by the same company — after observing stringent cleaning procedures of the weld region — showed high performance, achieving 24.5 MV/m (see figure 2.1.9). Later cavities made by the same company showed still better performance.

2.1.5.3 Diagnostic methods and quality control

The deficiencies encountered in the first series production of TTF cavities initiated the development of several diagnostic methods and quality control procedures.

Electron microscopy. Scanning electron microscopy with energy-dispersive X-ray analysis (EDX) is used to identify foreign elements on the surface. Only a depth of about 1 μm can be penetrated, so one has to remove layer by layer to determine the diffusion depth of titanium or other elements. The titanium layer applied in the high temperature treatment was found to extend to a depth of about 10 μm in the bulk niobium. The sensitivity of the EDX method is limited and a Ti fraction below 0.5 % is undetectable. Auger electron spectroscopy offers higher sensitivity and showed titanium migration at grain boundaries to a depth of 60 μm: hence a layer of this thickness must be removed from the RF surface by BCP after post-purification with Ti getter.

Eddy-current scan. Microscope methods are restricted to small samples and cannot be used to study entire cavities. In addition the methods are far too time-consuming to check large niobium sheets. A practical device for the quality control of all niobium sheets going into cavity production is a high-resolution eddy-current system developed at BAM. The apparatus operates similar to a turn table and permits a high scanning speed (about 10 minutes for a 260 mm diameter disk). A two-frequency principle is applied: scanning with high frequency (about 1 MHz) allows detection of surface irregularities, while the low frequency signal (about 150 kHz) is sensitive to bulk inclusions. The performance of the eddy-current scanning device was verified with a Nb test sheet containing implanted tantalum deposits of 0.2 to 1 mm diameter.

2.1.5.4 Second and third series of TTF cavities

The niobium sheets were all eddy-current scanned to eliminate material with tantalum or other foreign inclusions before the deep drawing of half cells. More than 95 % of the sheets were found free of defects, the remaining ones showed grinding marks, imprints from rolling or large signals due to small iron chips. Most of the rejected sheets were recoverable by applying some chemical etching. The eddy-current check has proven to be an important quality control procedure, not only for the cavity manufacturer but also for the supplier of the niobium sheets.

Stringent requirements were imposed on the electron-beam welding procedure to prevent the degraded performance at the equator welds encountered in the first series. After mechanical trimming, the weld regions were cleaned by a light chemical etching followed by ultra-pure water rinsing and clean-room drying. The cleaning process was performed not more than 8 hours in advance of the EB welding.

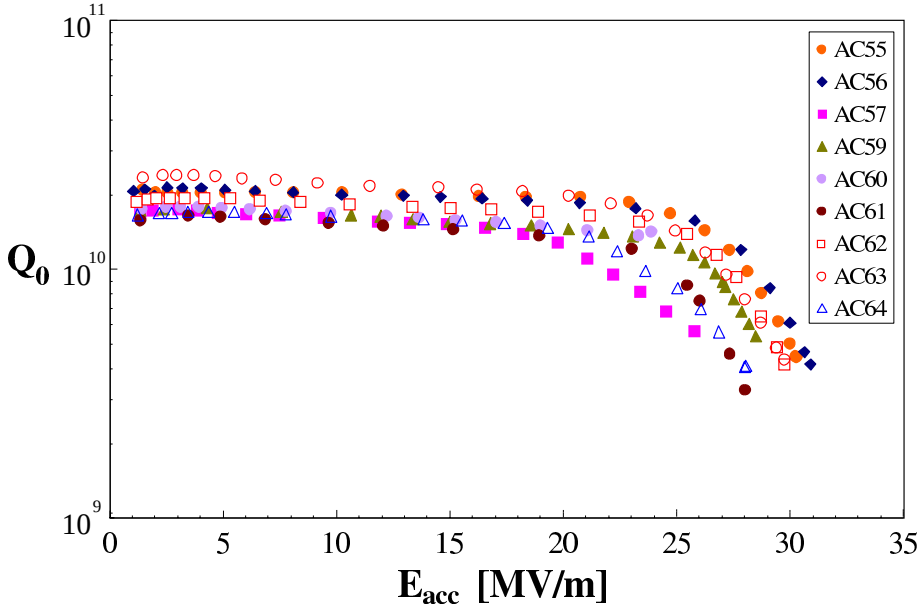

Figure 2.1.10: *Excitation curves of cavities of the third production series.*

Since implementing these two additional quality control measures, no foreign material inclusions nor weld contaminations have been found in new cavities tested so far.

2.1.5.5 Test results in vertical cryostat

All new cavities were subjected to the standard treatment described in section 2.1.4.3, including the post-purification with titanium getter at 1400°C. In the second series there was one cavity with a serious weld defect (a repaired hole in an equator weld). The average gradient of the remainder is $23.3 \pm 2.3\,\mathrm{MV/m}$ at $Q_0 \geq 1 \cdot 10^{10}$. From the third series (produced by one company), nine cavities have been tested to date (see figure 2.1.10). They exceed the TESLA-500 specification: the average gradient at $Q_0 \geq 1 \cdot 10^{10}$ is $26.1 \pm 2.3\,\mathrm{MV/m}$ and the average quality factor at the design gradient of $23.4\,\mathrm{MV/m}$ is $Q_0 = (1.39 \pm 0.35) \cdot 10^{10}$.

As of writing, five cryogenic modules each containing eight 9-cell resonators have been assembled. Figure 2.1.11 shows the performance of the cavities in the three production series and of those installed in the five cryomodules. In both cases the average gradient exhibits a clear trend towards higher values, and the spread in gradient across the cavities (as indicated by the error bars) is shrinking. The most recent cavities exceed the $23.4\,\mathrm{MV/m}$ operating gradient of TESLA-500 by a comfortable margin.

2.1.5.6 Tests with main power coupler in horizontal cryostat

After having passed the acceptance test in the vertical bath cryostat, the cavities are welded into their liquid helium container and equipped with the main power coupler.

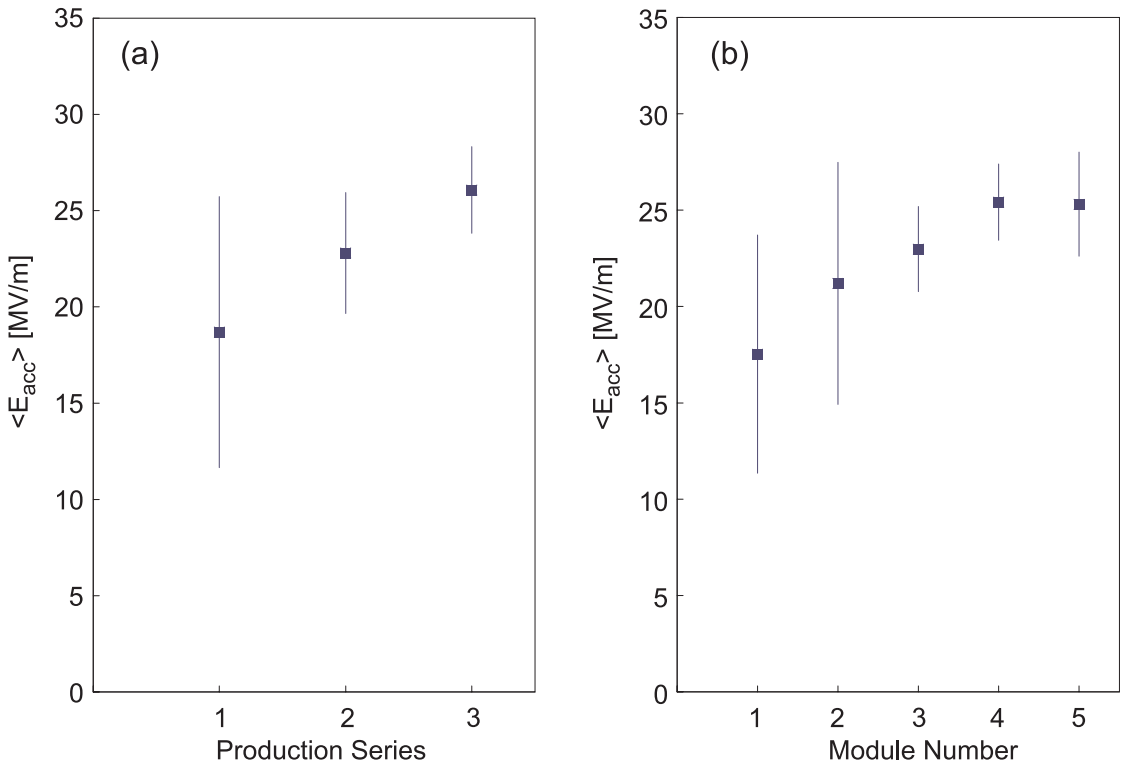

Figure 2.1.11: *Average accelerating gradients at $Q_0 \geq 10^{10}$ measured in the vertical test cryostat of: (a) the cavities in the three production series; and (b) the cavities installed in the first five cryogenic modules for TTF (see also [9]).*

The power coupler is adjusted to an give an external Q[1] of typically $3 \cdot 10^6$. The accelerating fields achieved in the vertical and the horizontal test are well correlated as shown in figure 2.1.12. In a few cases a reduced performance was seen, usually caused by field emission. Several cavities improved their performance in the horizontal test because of operation with short (millisecond) pulses[2] instead of the continuous wave (cw) operation in the vertical cryostat. The results show that the good performance of the cavities is maintained by taking care to avoid dust contamination during mounting of the helium vessel and power coupler.

In one of the cryomodules installed in the TTF linac the maximum usable gradient was determined for each of the eight cavities, restricted by a minimum quality factor of $1 \cdot 10^{10}$ to restrict the heat load on the helium system. The average gradient was 23.6 MV/m, indicating that installation of the individual cavities into a module does not degrade their performance.

[1] In the vertical test, a weakly coupled input antenna is used whose external Q is less than the Q_0 of the cavity.

[2] the addition of the main power coupler allows the use of short pulses.

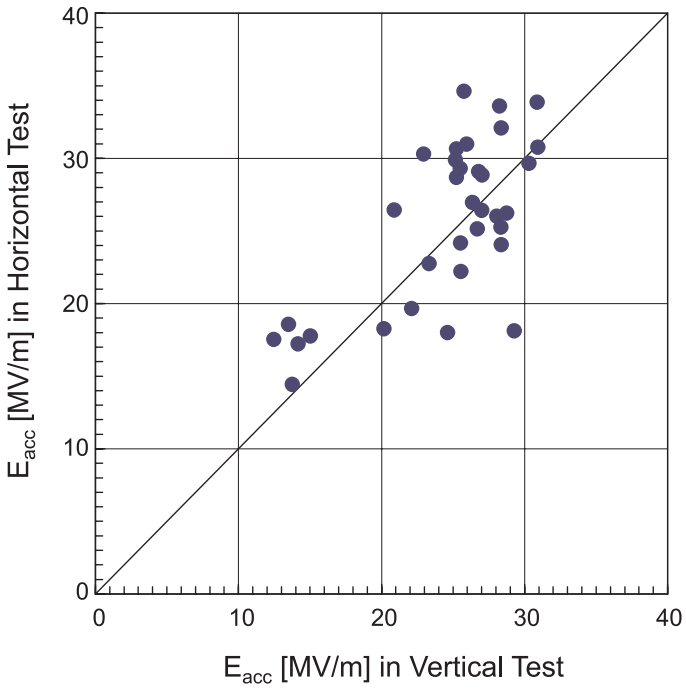

Figure 2.1.12: *Comparison of vertical and horizontal test results at 2 K. The average accelerating field achieved in the vertical test with continuous wave (cw) excitation is 24.5 MV/m, in the horizontal test with pulsed excitation 25.5 MV/m. The RF pulse has a rise time of 500 µs and a flat top of 800 µs.*

2.1.6 Cavities of ultimate performance

The design c.m. energy of 500 GeV corresponds a gradient of 23.4 MV/m in the present nine-cell cavities with a reduced beam pipe length. The cavities from the third industrial production exceed this value by a comfortable margin, and consequently TESLA-500 can be realized with the present cavity fabrication and preparation methods. The energy upgrade to 800 GeV (section 1.4) requires use of the so-called 'superstructure', where the effective acceleration length is increased by combining together several multicell cavities with reduced inter-cavity spacing (section 2.1.8). The accelerating field gradient required is then 35 MV/m, which represents a significant increase compared to the performance achieved so far. Three main obstacles might prevent us from approaching the superconductor limit of ≈ 50 MV/m in multicell niobium cavities:

- foreign material contamination in the niobium;
- insufficient quality and cleanliness of the inner RF surface; and
- quality of the welds.

The first two points are being addressed by on-going R&D programs (section 2.1.6.1). The feasibility of so-called 'seamless' cavities to avoid welding is also being investigated

(section 2.1.6.4).

While material problems may represent a significant challenge to achieving the required cavity performance for the 800 GeV upgrade, a fundamental limitation is given by the effect of Lorentz-force detuning, which must be reduced to allow efficient 35 MV/m operation in the linac (section 2.1.6.3).

2.1.6.1 Quality improvement of niobium and post-purification

As already discussed, niobium for microwave resonators has to be of extreme purity for two reasons: dissolved gases like hydrogen, oxygen and nitrogen impair the heat conductivity at liquid helium temperature; and contamination by normal-conducting or weakly superconducting clusters close to the RF surface may cause a premature breakdown of the superconducting state. The niobium for the TTF cavities was processed in industry with plants which are in addition used for other metals. For the large series production of cavities needed for the TESLA collider, it would be economical to install dedicated facilities for the niobium refinery and the forging and sheet rolling operations. A substantial improvement in material quality can be expected from specialized installations which are designed for the highest cleanliness, and which are free of contamination by other metals. The same applies for the electron-beam welding machines which must conform to Ultra High Vacuum standards: such a high-quality EB welding machine will be installed at DESY in early 2001 to be used in the cavity R&D program.

The recent TTF cavities have been made from eddy-current checked niobium with gas contents in the few ppm range and an RRR of 300. Ten 9-cell cavities have been tested before and after the 1400°C heat treatment which raises the RRR to more than 500. The average gain in gradient was 4 MV/m. The result implies that, with the present surface preparation by chemical etching, the heat treatment is an indispensable step in achieving the TESLA-500 goal. From tests at KEK there is some evidence that the tedious and costly 1400°C heat treatment may not be needed in cavities prepared by electropolishing (see below).

2.1.6.2 Electrolytic polishing (electropolishing)

The Buffered Chemical Polishing (BCP) used at TTF to remove a 100–200 μm thick damage layer produces a rough niobium surface with strong grain boundary etching. An alternative method is 'electropolishing' (EP) in which the material is removed in an acid mixture under current flow. Sharp edges and burrs are smoothed out and a very glossy surface can be obtained. In figure 2.1.13 BCP and EP treated niobium samples are compared.

Electropolishing of niobium has been already used in the 1970's to obtain high magnetic surface fields in small X-band cavities (see references in [6]). But it is only recently that this method has been developed to a high standard at the KEK laboratory in Japan [10]. The electrolyte is a mixture of H_2SO_4 (95 %) and HF (46 %) in a volume ratio of 9:1. The bath temperature is 30–40°C. The process consists of two alternating steps [11, 6]: oxidation of the niobium surface by the sulphuric acid under current flow

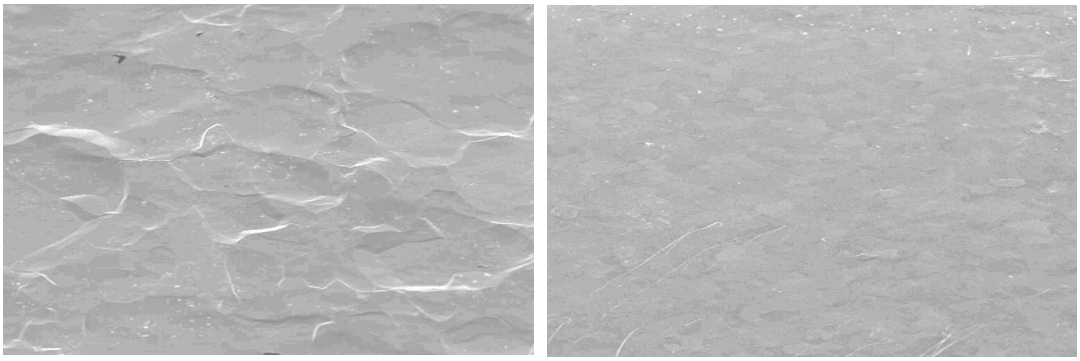

Figure 2.1.13: *SEM micrographs of niobium surface after BCP (left) and EP (right). The average surface roughness is 1 μm in the left and 0.1 μm in the right sample. Height of micrograph is 500 μm (Courtesy of CERN).*

(current density about 500 A/m^2); and dissolving of the Nb_2O_5 by the hydrofluoric acid. The rate of material removal is around 40 μm per hour.

Since 1995 gradients above 35 MV/m have been routinely obtained at KEK in several electropolished L-band single-cell niobium cavities [12]. Most of these cavities were made from *RRR* 200 material and not subjected to a high temperature heat treatment for post-purification. A KEK-Saclay collaboration demonstrated that EP raised the accelerating field of a 1-cell cavity by more than 7 MV/m with respect to BCP. When the electropolished surface was subjected to a subsequent BCP, the cavity suffered a clear degradation in RF performance which could be recovered by a new EP [13]. Thus there is strong evidence that EP is the superior surface treatment method.

CERN, DESY, KEK and Saclay started a joint R&D program with EP of half cells and 1-cell cavities in August 1998. Gradients between 35 and 42 MV/m are now routinely being achieved [14] (see figure 2.1.14). The current program focuses on cavities made from niobium with $RRR = 300$. An important goal is to determine whether or not the high gradients so far achieved can be obtained without the time-consuming 1400°C heat treatment.

Recently it has been found that an in-situ baking of the evacuated cavity at 100–150°C (following the EP and clean water rinsing) is an essential step in reaching higher gradients without a strong degradation in quality factor [15]. The underlying mechanism is not yet understood. The baking was applied to all single-cell cavities.

The transfer of the EP technique to multicell cavities requires considerable investment. In a first test a 9-cell TESLA resonator has been electropolished by a Japanese company, improving its performance from 22 to 32 MV/m (figure 2.1.15). An EP facility for 9-cell cavities is under construction at DESY. Given the results obtained so far, it is likely that EP will form an essential part of producing cavities capable of achieving the 35 MV/m operating gradient needed for TESLA-800.

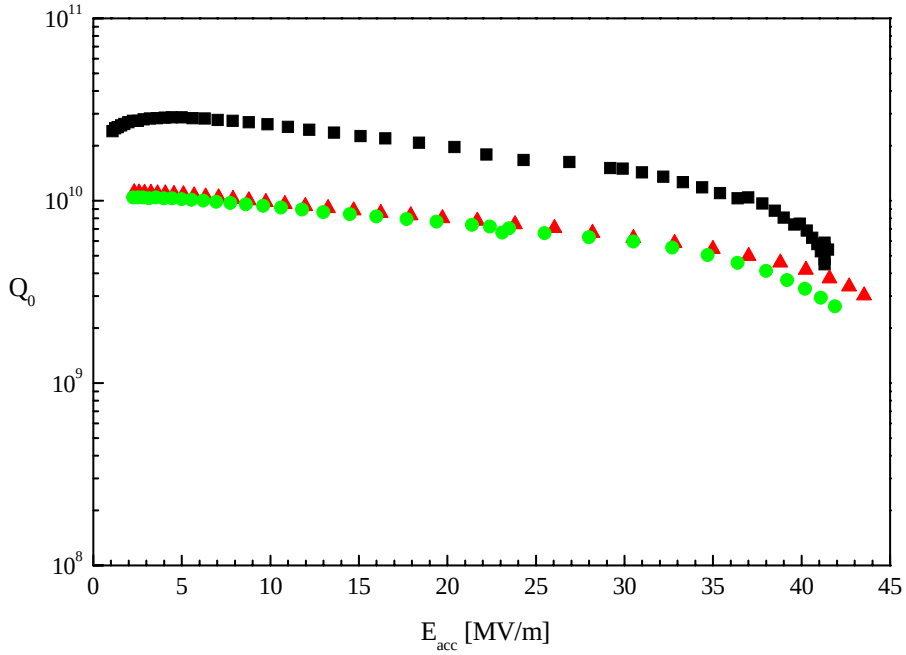

Figure 2.1.14: *Excitation curves of three electropolished single-cell cavities without heat treatment at 1400° C. The tests have been performed in different cryostats and under slightly different conditions (magnetic shielding, helium temperature).*

2.1.6.3 Frequency stability of the cavities

The pulsed operation leads to a time-dependent frequency shift of the 9-cell cavities. The stiffening rings joining neighbouring cells are adequate to keep this 'Lorentz-force detuning' within tolerable limits up to the nominal TESLA-500 gradient of 23.4 MV/m. To allow for higher gradients the stiffening must be improved[1], or alternatively, the cavity deformation must be compensated. The latter approach has been successfully demonstrated using a piezoelectric tuner [17] (see figure 2.1.16). The result indicates that the present stiffening rings augmented by a piezoelectric tuning system will permit efficient cavity operation at the TESLA-800 gradient of 35 MV/m.

2.1.6.4 Seamless cavities

To explore the feasibility of cavities without weld connections in the regions of high electric or magnetic RF fields, the TESLA collaboration has pursued two alternative 'seamless' production methods: spinning and hydroforming.

Spinning. At the Legnaro National Laboratory of INFN in Italy, the spinning technique [18] has been used to deform flat niobium disks into 1.3 GHz cavities. A very high degree of material deformation was needed, leading to a rough inner cavity

[1] The reinforcement of niobium cavities by a plasma-sprayed outer copper layer has been investigated at Orsay [16].

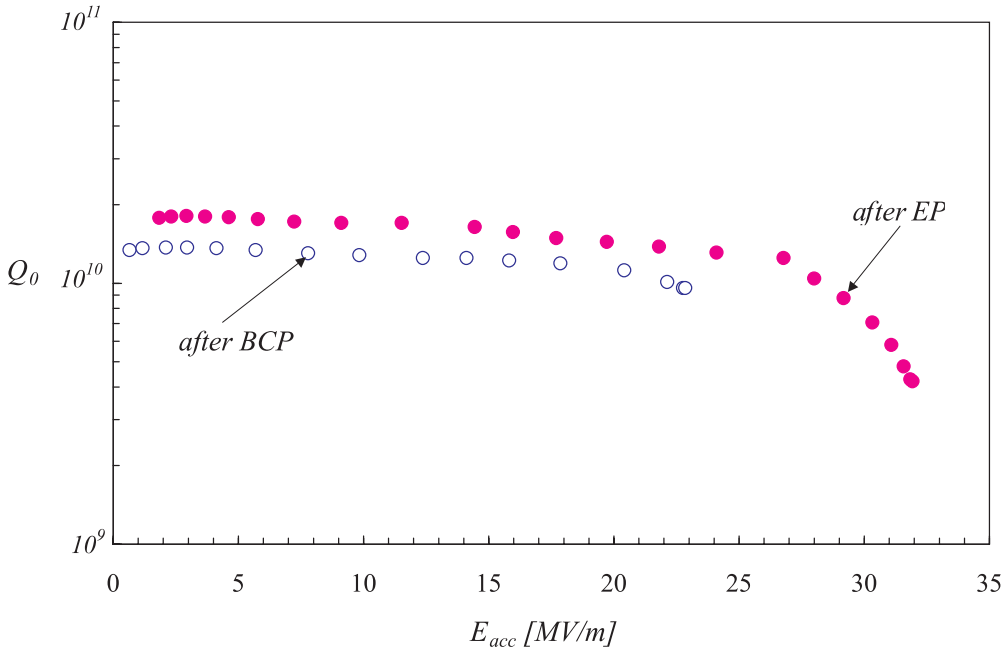

Figure 2.1.15: *Excitation curve of a TESLA 9-cell cavity after buffered chemical polishing (BCP) and electropolishing (EP), but before application of the baking procedure.*

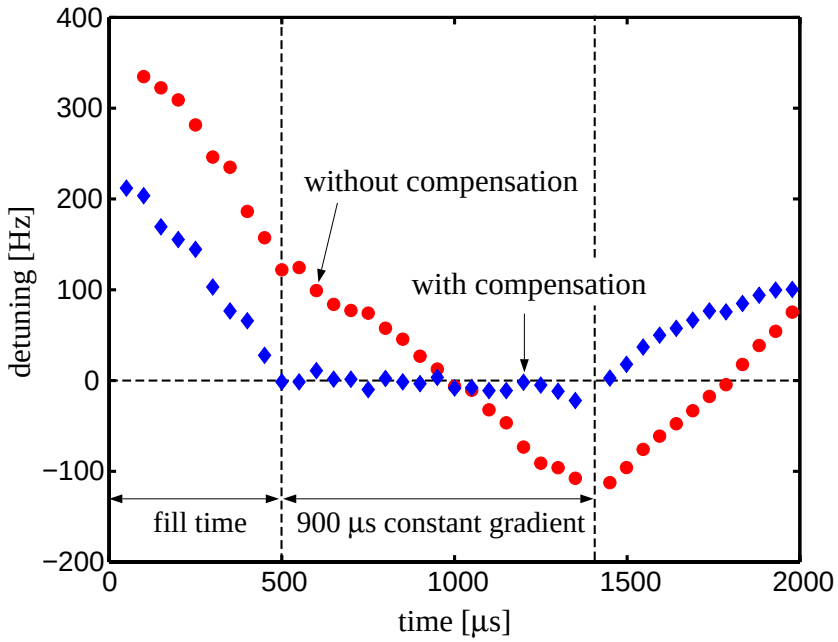

Figure 2.1.16: *Piezoelectric compensation of the Lorentz-force induced frequency shift in pulsed-mode cavity operation. The accelerating field is 23.5 MV/m.*

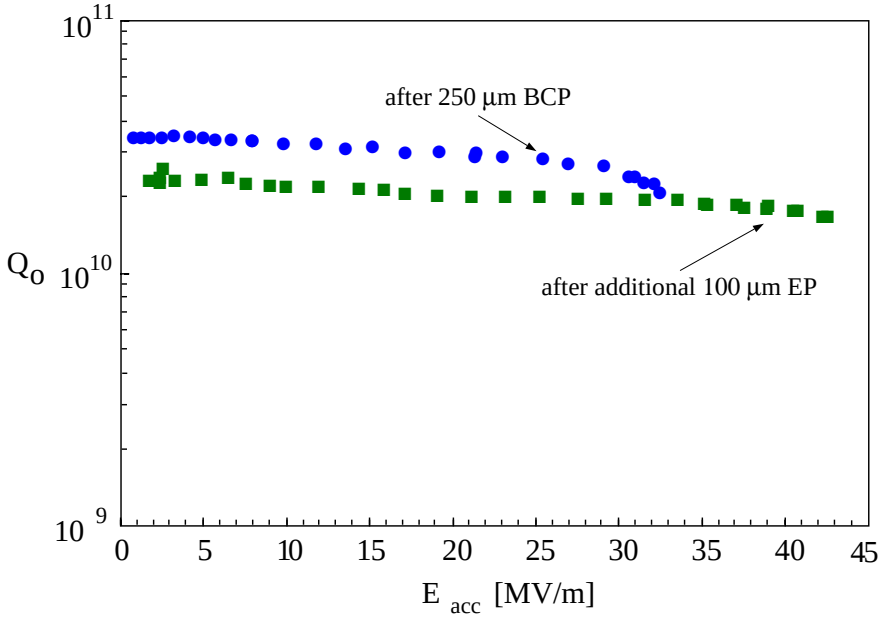

Figure 2.1.17: *Excitation curve of a hydroformed 1-cell cavity after BCP and EP. Preparation and measurement of the cavity was carried out by P. Kneisel at Jefferson Laboratory.*

surface. After mechanical grinding and heavy etching (removal of more than 500 μm), gradients of the order of 25 MV/m were obtained [20]. With an electropolished cavity, up to 38 MV/m have been achieved [19]. Presently 1-cell, 3-cell and 9-cell cavities are being produced from seamless Nb tubes with an *RRR* of 300; in this case the amount of deformation will be much less and a smoother inner surface can be expected.

Hydroforming. The deformation of a seamless niobium tube into a cavity by hydrostatic pressure is being studied in collaboration with industry. Starting from a tube of intermediate diameter, the first step is to reduce the diameter at the iris and then to expand the tube in the equator region. The deformation process is first modeled on a computer, using measured strain-stress and plastic flow characteristics of the niobium tubes to be used. The shaping of the tube into an external mould is done under computer control by applying internal over-pressure and at the same time compression along the axis direction. The deformation is done in small steps with a strain rate below 10^{-3}/s, following the procedure established in the simulation.

Two cavities were hydroformed at DESY from *RRR* 100 tubes of 134 mm diameter and 2 mm wall thickness. One cavity was produced at a company (Butting) from a deep drawn *RRR* 200 niobium tube of 156 mm diameter and 3 mm thickness. An intermediate annealing was not needed. The DESY cavities were post-purified at a temperature of 1400°C with titanium getter, increasing the *RRR* to more than 300. They achieved accelerating fields of 33 and 32 MV/m respectively at $Q_0 = 2 \cdot 10^{10}$. One cavity was then electropolished at KEK (removing 100 μm) and reached the record

value[1] of $E_{acc} = 42\,\mathrm{MV/m}$ [21] (see figure 2.1.17). The most remarkable observation is that the excitation curve $Q_0(E)$ is almost flat up to the highest field.

2.1.6.5 Niobium sputtered cavities

Recent investigations at CERN [22] and Saclay [23] have shown that 1.3–1.5 GHz single-cell copper cavities with a niobium sputter layer of about 1 μm thickness are able to reach accelerating fields in the order of 20–25 MV/m. This is a considerable improvement in comparison with the LEP cavities but still almost a factor of two below the performance of solid niobium cavities. Moreover the quality factor is continuously decreasing with rising gradient. At present there is no experimental evidence to suggest that Nb sputtered copper cavities have the potential of achieving the TESLA-800 goal.

2.1.7 Auxiliary systems and components

2.1.7.1 Helium vessel and tuning system

The cavity is welded into a cylindrical vessel which contains the superfluid helium needed for cooling and serves as part of the tuning mechanism. The tank is made from titanium whose thermal contraction is almost identical to that of niobium. A titanium bellows allows the length to be adjusted by the mechanical tuner.

Tuning the cavity to its nominal operating frequency is a challenging task since the cavity length must be adjusted with sub-micron accuracy. The tuning system used at TTF consists of a stepping motor with a gear box and a double lever arm. The moving parts operate at 2 K in vacuum. The frequency tuning range is ± 300 kHz with a resolution of 1 Hz. The tuners in the TTF linac have been working for two years with high reliability. For TESLA a more compact tuning system is under development which incorporates a piezoelectric crystal for fast frequency adjustment (feedback).

2.1.7.2 Main power coupler

For TTF several coaxial power input couplers have been developed [24, 25, 26, 27, 28], consisting of a cold section which is mounted on the cavity in the clean room and closed by a ceramic window, and a warm section which contains the transition from the coaxial line to the waveguide. The latter part is evacuated and sealed against the air-filled wave guide (WR 650) by a second ceramic window (see figure 2.1.18). The elaborate two-window solution was chosen for protection of the cavity against contamination during mounting in the cryomodule, and against a window fracture during linac operation.

Bellows in the inner and outer conductors of the coaxial line of the coupler allow a few mm of motion between the cold mass and the vacuum vessel when the cavities are cooled from room temperature to 2 K. A low thermal conductivity is achieved by using stainless steel pipes and bellows with a 10–20 μm copper plating at the radio frequency surface. Lower values than the design heat loads of 6 W at 70 K, 0.5 W at 5 K and 0.06 W at 2 K have been achieved in practice.

[1] as of writing

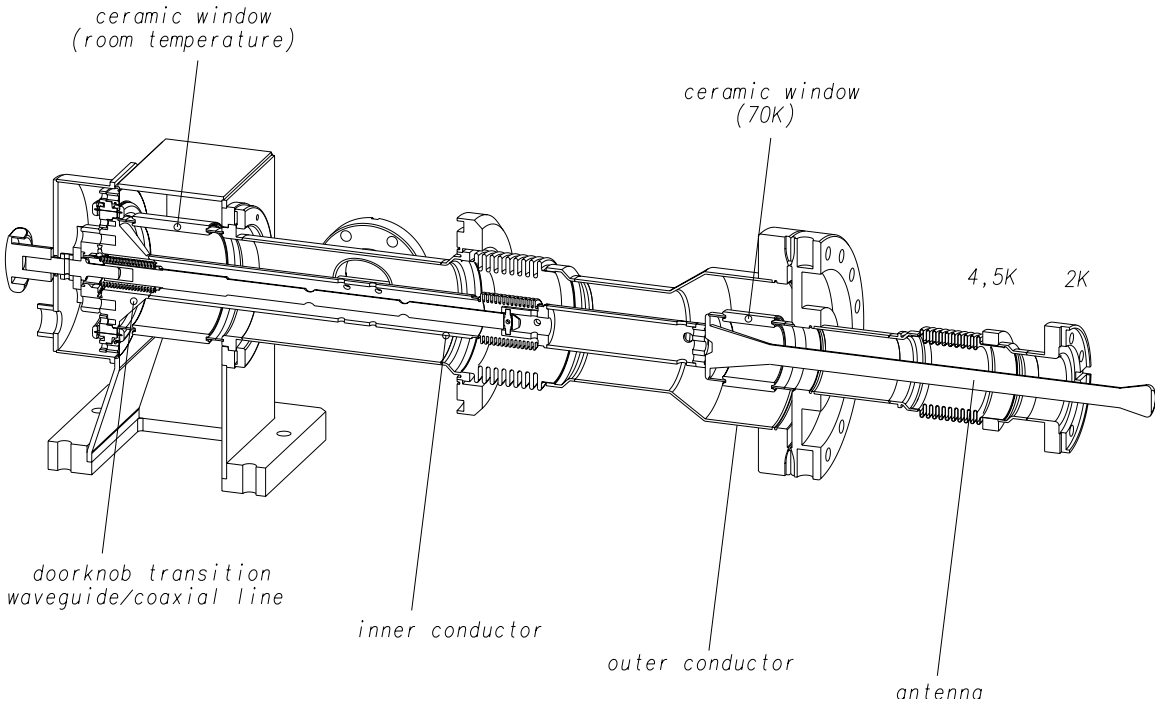

Figure 2.1.18: *The coaxial power input coupler (version III) for the TTF cavities. The coaxial part is thermally connected to the 4.5 K and 70 K radiation shields of the cryostat. The input antenna is movable to vary Q_{ext} in the range* $(1-6)\cdot 10^6$.

The most recent coupler (version III) features two cylindrical Al_2O_3 windows which are insensitive to multipacting resonances [29], and are coated with titanium nitride to reduce the secondary electron emission coefficient [30]. The coaxial line is also insensitive to multipacting resonances, and a further suppression is achieved by applying a dc bias voltage (up to 5 kV) to the inner conductor; such a bias was originally proposed at INP Novosibirsk and has proven very beneficial in the case of the LEP couplers [31].

An instantaneous power of 230 kW has to be transmitted to provide a gradient of 23.4 MV/m for a 950 μs long beam pulse of 9.5 mA. The filling time of the cavity amounts to 420 μs, and the decay time (after the beam pulse) is an additional 500 μs. The external quality factor of the coupler is $Q_{ext} = 2.5\cdot 10^6$ at 23.4 MV/m. By moving the inner conductor of the coaxial line, Q_{ext} can be varied in the range (1–6)$\cdot 10^6$ to cope with different beam loading conditions and to facilitate an in-situ high power processing of the cavities at RF power levels up to 1 MW. This feature has proven extremely useful on several occasions to eliminate field emitters that entered the cavities at the last assembly stage.

All couplers needed some conditioning but then performed according to specification. During experimental tests at TTF, the couplers were able to transmit up to 1.5 MW of RF power in travelling wave mode.

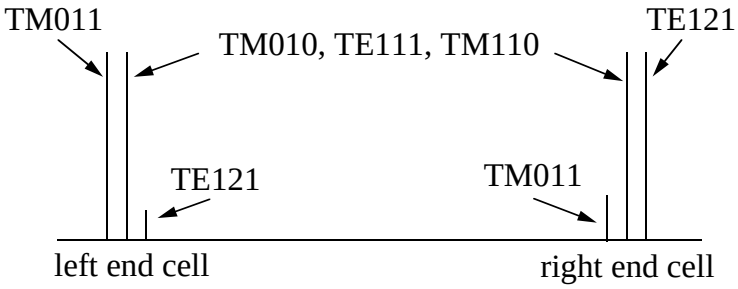

Figure 2.1.19: *Effect of asymmetric end cell shaping on various modes. The main accelerating mode TM_{010} and the higher modes TE_{111} and TM_{110} are not affected while TM_{011} is enhanced in the left end cell, TE_{121} in the right end cell. Using HOM couplers at both ends, all higher-order modes can be extracted.*

2.1.7.3 Higher-order mode couplers

The intense electron bunches excite eigenmodes of higher frequency in the resonator which must be damped to avoid multibunch instabilities and beam breakup. This is accomplished by extracting the stored energy via higher-order mode (HOM) couplers mounted on the beam pipe sections of the nine-cell resonator. A problem arises from 'trapped modes' which are concentrated in the centre cells and have a low field amplitude in the end cells. An example is the TE_{121} mode. By an asymmetric shaping of the end half cells one can enhance the field amplitude of the TE_{121} mode in one end cell, while preserving the field homogeneity of the fundamental mode and the good HOM coupling to the untrapped modes TE_{111}, TM_{110} and TM_{011}. The effects of asymmetric end cell tuning are sketched in figure 2.1.19.

The two polarization states of dipole modes in principle require two orthogonal HOM couplers at each side of the cavity. In a string of cavities this complexity can be avoided since the task of the 'orthogonal' HOM coupler is taken over by the HOM coupler of the neighboring cavity. The design of the HOM coupler is shown in figure 2.1.20. The superconducting pickup antenna is well cooled and insensitive to γ radiation and electron bombardment. A tunable 1.3 GHz notch filter suppresses power extraction from the accelerating mode to less than 50 mW at 23.4 MV/m.

2.1.8 The superstructure concept

2.1.8.1 Limitation on number of cells per cavity

A fundamental design goal for a linear collider is to maximize the active acceleration length in the machine and to reduce the cost of the radio frequency system. Hence it is desirable to use accelerating structures with as many cells as possible both to increase the filling factor and to reduce the number of power couplers and wave guide components. However, the number of cells per cavity (N) is limited by the conditions of field homogeneity and the presence of trapped modes. For a standing-wave structure

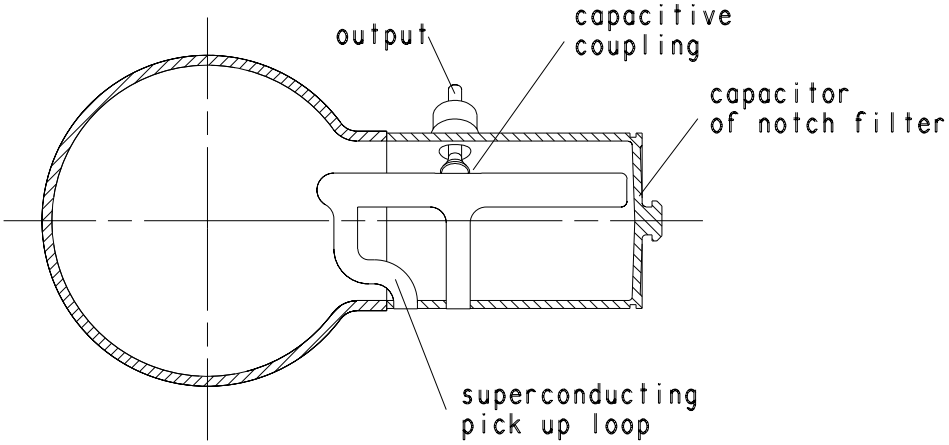

Figure 2.1.20: *Cross-section of the higher order mode (HOM) coupler.*

operated in the π-mode, a frequency error δf in an individual cell results in an error in the accelerating field amplitude (δA_{cell}) of

$$\delta A_{cell} \propto \frac{N^2\,\delta f}{k_{cc}},$$

where k_{cc} is the cell-to-cell coupling. The sensitivity of the field pattern to small perturbations grows quadratically with the number of cells. The probability of trapping higher-order modes within a structure also increases with N; such modes with a small field amplitude in the end cells are difficult to extract by the HOM couplers. In superconducting cavities these modes are particularly dangerous because of their long damping times: the modes persist over a significant portion of the bunch train, causing emittance dilution (beam break-up, see section 3.2).

The 9-cell structure chosen for TESLA is a good compromise between the conflicting requirements of optimum filling factor, field homogeneity and absence of trapped modes. In the TESLA Test facility linac each cavity is equipped with its own input coupler and tuning system. The cavities are connected by beam tube sections and bellows with a total length of $3/2\,\lambda$, where $\lambda = 0.223\,\mathrm{m}$ is the RF wavelength. The tube diameter (78 mm) is below cutoff for 1.3 GHz: hence there is no power flow from one cavity to the next. For the baseline design of TESLA-500 the 9-cell cavity concept with individual power coupler is maintained, but the interconnection is shortened to improve the filling factor of the machine and to reduce the nominal accelerating gradient from 25 to 23.4 MV/m.

2.1.8.2 The superstructure

The limitations on the number of cells per cavity can be circumvented by joining several multicell cavities to form a so-called superstructure [32]. Short tubes of sufficient diameter (114 mm) enable power flow from one cavity to the next. Two types of

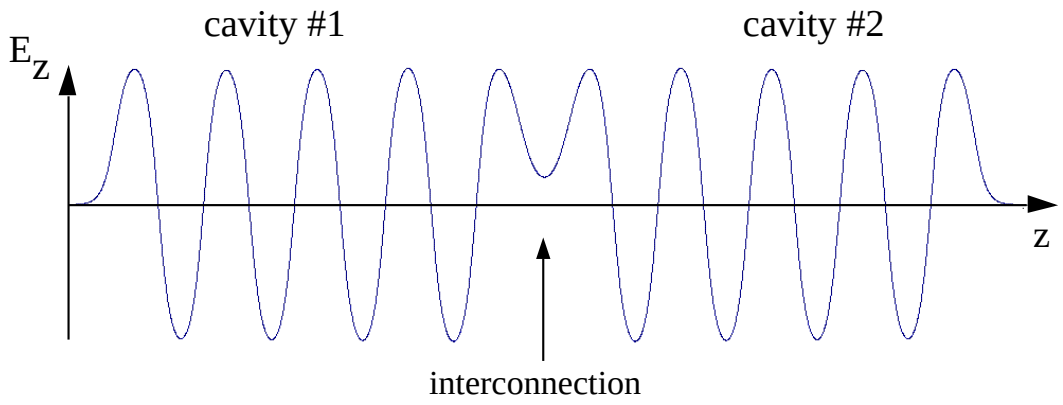

Figure 2.1.21: *E_{acc} along the axis of a 2×9-cell superstructure.*

superstructures have been investigated in detail: Superstructure I consisting or four 7-cell resonators; and, more recently, Superstructure II consisting of two 9-cell resonators. The chain of cavities is powered by a single input coupler mounted at one end. HOM couplers are located at the interconnections and at the ends. All cavities are equipped with their own tuners. The cell-to-cell coupling is $k_{cc} = 1.9\,\%$, while the coupling between two adjacent cavities is a superstructure is two orders of magnitude smaller at $k_{ss} \approx 3 \cdot 10^{-4}$: due to this comparatively weak inter-cavity coupling the issues of field homogeneity and HOM damping are much less of a problem than in a single long cavity with $N = 28$ or 18 cells. The shape of the centre cells is identical to those in the 9-cell TTF structures while the end cells have been redesigned to accommodate the larger aperture of the beam tube. The radio frequency properties of both superstructures are summarised in table 2.1.3.

2.1.8.3 Electrical properties of a superstructure

Field profile. Synchronism between the relativistic bunches and the accelerating field requires a length of $\lambda/2$ for the shortest interconnection. When N is an odd number, the (π-0) mode (cell-to-cell phase advance is π and cavity-to-cavity phase advance is zero) can be used for acceleration. The field profile of this mode is shown in figure 2.1.21.

The cavities are tuned to equal field amplitude in all cells and are then welded into their liquid helium tanks and joined to form the superstructure. It has been verified that the pre-tuning of the cavities can be preserved during the assembly steps. The equalisation of the field amplitudes across the cavities is then accomplished by a method resembling the standard bead pull technique used to homogenise the field in a multicell cavity. By means of the mechanical tuners the cavities are changed in volume one after the other by a given amount and the resulting frequency shifts of the (π-0) mode recorded. A perturbation calculation allows the required adjustments to be determined. The method has been validated by tests using a copper model of the superstructure and by computer simulations. The tuning can be carried out on the cleaned and evacuated superstructure, and requires only one pickup probe for all the

Parameter	4×7cell	2×9cell
sensitivity factor, N^2/k_{cc}	2600	4300
cell-to-cell coupling k_{cc}	1.9 %	1.9 %
cavity-to-cavity coupl. k_{ss}	$3.6\cdot 10^{-4}$	$2.8\cdot 10^{-4}$
(R/Q) cavity	736 Ω	986 Ω
E_{peak}/E_{acc}	2.0	2.0
B_{peak}/E_{acc}	4.18 $\frac{\text{mT}}{\text{MV/m}}$	4.18 $\frac{\text{mT}}{\text{MV/m}}$
distance to next resonance	158 kHz	330 kHz

Table 2.1.3: *RF parameters of the superstructures.*

cells.

Induced energy spread in a bunched beam. The main concerns for a chain of cavities fed by a single input coupler is the flow of the RF power through the interconnecting beam pipes, and the time needed to reach equal field amplitude in all cells during pulsed-mode operation. The power flow has been extensively studied [33, 34] with two independent codes, HOMDYN and MAFIA. The relative spread in energy gain in a train of 2820 bunches is predicted to be less than 10^{-4} (figure 2.1.22), indicating that the energy flow is sufficient to refill the cells in the time interval between two adjacent bunches.

In superstructure I (4×7 cells) the main power coupler must transmit 675 kW of travelling wave power at 500 GeV c.m. energy and 1080 kW at 800 GeV. For Superstructure II (2×9 cells) the numbers are 437 kW and 705 kW, respectively. The TTF couplers have been tested up to 1500 kW and are therefore sufficient to feed either type of superstructure. To provide an additional safety margin for the operation at 35 MV/m (TESLA-800) the diameter of the cold coupler section will be increased from 40 mm to 60 mm.

The higher-order modes have been extensively studied for Superstructure I. Nearly all modes propagate through the 114 mm diameter beam pipe and are efficiently damped with 5 HOM couplers mounted at the three interconnections and at both end tubes. The details of the dipole mode impedances differ somewhat from the 9-cell cavity, but the overall effect on the beam dynamics is similar [35].

2.1.8.4 Technical and economical aspects of the superstructures

The baseline design of TESLA-500 rests on the well-established 9-cell TTF cavity technology with individual power couplers but a reduced length of the interconnection (283 mm instead of 346 mm for beam pipes and bellows). The two superstructures under consideration improve the filling factor by 6 % and require a factor of 2–3 fewer main power couplers in the machine. Keeping the total length of the collider constant, the superstructures allow us to reach the 500 GeV c.m. energy with a gradient of 22 MV/m, compared to 23.4 MV/m with individual 9-cell cavities. In table 2.1.4 the important parameters of the three versions of the TESLA accelerating system are

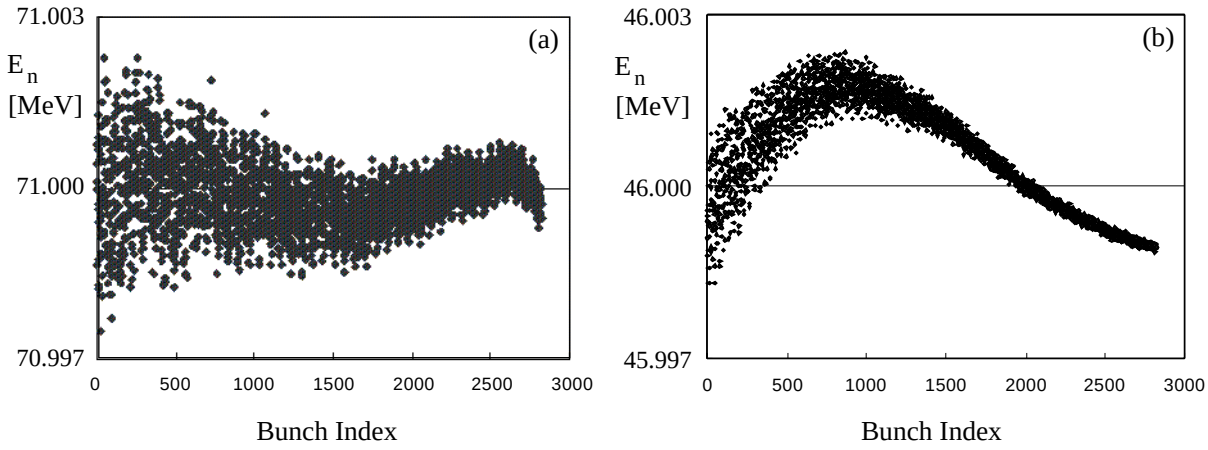

Figure 2.1.22: *Computed energy gain E_n for a train of 2820 bunches in: (a) Superstructure I (nominal gain 71 MeV); and (b) Superstructure II (nominal gain 46 MeV).*

Layout	L_{active} [m]	E_{acc} [MV/m]	no. of power coupl.	no. of HOM coupl.	no. of tuners	filling factor L_{active}/L_{total} [%]	P_{trans} [kW]
9-cell	1.04	23.4	20592	41184	20592	78.6	232
4×7-cell	3.23	22.0	7032	35160	28128	84.9	675
2×9-cell	2.08	22.0	10926	32778	21852	84.8	437

Table 2.1.4: *Different layouts of the TESLA accelerating system. The numbers refer to TESLA-500. P_{trans} is the power per RF coupler transmitted to a 9.5 mA beam.*

compared.

Superstructure I. The 4×7-cell structure appears most attractive in terms of cost reduction: 7000 superstructures would be needed and the same number of power couplers. On the other hand, the cavity comprises of only 7 cells, so the number of helium vessels and tuning systems is higher than with 9-cell cavities. A clear disadvantage is the large overall length of 3.86 m which makes chemical and heat treatments of the entire structure difficult.

Superstructure I was proposed first and extensive RF measurements have been performed on a copper model. A niobium prototype is in preparation for a beam test in the TTF linac. In this prototype the 7-cell cavities are joined by superconducting flanges. The third generation of TTF input coupler and five HOM couplers will be

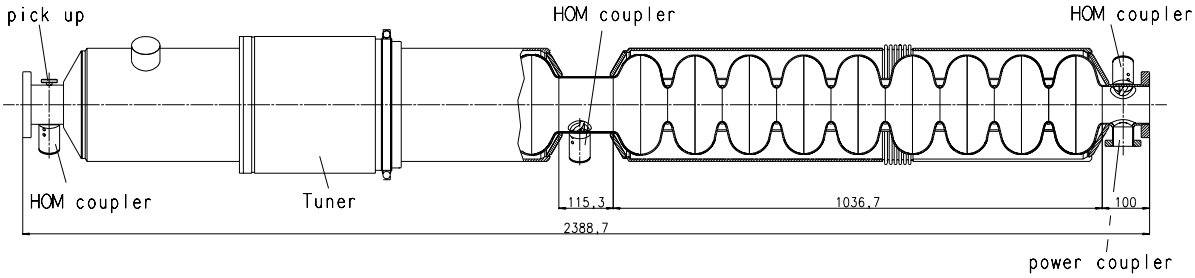

Figure 2.1.23: *Superstructure II consisting of two 9-cell resonators joined by a 114 mm diameter beam pipe.*

used. The beam test is scheduled for beginning of 2002 and will help verify the energy spread computations and the RF measurements on the copper model. In addition the performance of the HOM couplers, which are exposed to a higher magnetic field due to the enlarged beam tube diameter, can be tested. Another goal is to validate the proposed tuning method when the structure is installed in the linac.

Superstructure II. The combination of two 9-cell resonators (see figure 2.1.23) achieves the same high filling factor[1] of 85 % but is only 2.39 m long. This structure can be chemically treated and handled with an upgraded version of the facilities at TTF. Therefore no new welding and preparation techniques will be needed for the assembly, which means that the excellent performance obtained with the single 9-cell cavities can also be expected from the superstructure. Electropolishing of the 2.39 m long unit should also be possible. The only disadvantage in comparison with superstructure I is the higher number of power couplers, but this has to be balanced against the lower number of tuners and helium vessels. Superstructure II will need about eighteen months of R&D before it can go into series production: as of writing, it is expected to become the preferred solution for the TESLA collider.

2.1.9 Summary of TESLA acceleration system layout

In this section we briefly summarize the layout of the superconducting cavity system for TESLA. Details can be found in the previous sections.

Baseline design. TESLA-500 can be safely realized using the existing 9-cell TTF cavities with a reduced length of the interconnecting beam pipes. In the third series of industrially produced cavities for TTF the required accelerating field of 23.4 MV/m is exceeded by an ample safety margin. Each of the cavities is equipped with its own power coupler. The couplers built for TTF can transmit far higher RF power levels than needed for the TESLA-500 beams. It should be noted that cavities, couplers and other auxiliary systems like helium vessel, frequency tuner and HOM couplers have been thoroughly tested with beam in the TTF linac and are suitable for the TESLA

[1] The filling factor defined here does not include additional lengths for magnets and module interconnections.

collider.

Improvement in surface quality by electropolishing. The essential step towards TESLA-800 is a new preparation method: the present chemical etching of the inner cavity surface will be replaced by electropolishing which leads to a much smoother surface. An electropolishing apparatus for 9-cell cavities and 2×9-cell superstructures is under development at DESY. According to numerous tests with 1-cell cavities, improved performance can be expected from the new technique with gradients in the 35–40 MV/m regime.

Superstructure. The active acceleration length in the TESLA machine can be increased by 6 % when two 9-cell cavities are joined by a very short beam pipe to form a superstructure. The nominal gradient for TESLA-500 is thereby reduced to 22 MV/m. Only one power coupler per superstructure is needed, resulting in a factor of two saving in power couplers and other wave guide components. About 18 months of R&D are required to make this option ready for series production.

The TESLA cavity system. The basic acceleration unit for TESLA will most likely be the 2×9-cell superstructure with a surface preparation by electrolytic polishing. According to present knowledge the TESLA-800 operating gradient should be safely achievable. The auxiliary components and systems (e.g. main power and HOM couplers, tuners) developed for TTF are already adequate for TESLA-500 and need only moderate improvement for TESLA-800. The TTF cavity stiffening scheme combined with a piezo-electric tuner will provide sufficient frequency stability at the TESLA-800 gradient of 35 MV/m.

Currently only cavities made from solid niobium offer the potential for achieving gradients of 35 MV/m, and this is the technology of choice for TESLA.

2.2 Integrated System Test

2.2.1 TESLA Test Facility — overview

The major challenge for the TESLA collaboration was to prove the feasibility and reliability of achieving accelerating gradients well above 20 MV/m, i.e. high enough for the 500 GeV linear collider. The TESLA Test Facility linac (TTFL) at DESY was constructed to show that the high gradients achieved in the cavities could be maintained during assembly into a linac test string, and then successfully operated with auxiliary systems to accelerate an electron beam to a few hundred MeV. The basic characteristics of the TTFL were designed to be as consistent as possible with the parameters of the TESLA linear collider design.

The original proposal for the TTF [36] was for a linac test string of four cryogenic modules, each containing eight superconducting nine-cell TESLA structures. The initial design goal was 15 MV/m, which was at that time substantially higher than superconducting cavities operated at other accelerator laboratories. Shortly after finishing the first design of the TTFL, it became clear that the test linac would be almost ideal to drive a Free Electron Laser (FEL) based on the principle of Self Amplified Spontaneous Emission (SASE): therefore the overall layout was changed and the FEL became

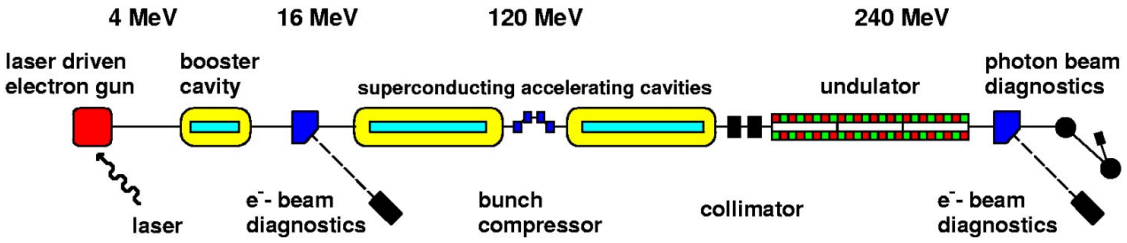

Figure 2.2.1: *Schematic layout of the TESLA Test Facility Linac (TTFL). The total length is ∼120 m.*

part of the TTF project [37, 38].

The TTF (linac) programme for the accelerator modules was planned to check many of the aspects of operation in the linear collider:

- gradient achievable in a standard linac module;
- input coupler and higher-order mode (HOM) coupler performance;
- radio frequency (RF) control of multi-cavity systems;
- Lorentz force detuning and microphonic noise effects;
- RF conditioning of cavities and couplers;
- vacuum performance / failure recovery potential;
- cryostat design and cryogenic operation / heat load;
- dark current;
- energy and beam position feedback and control;
- alignment.

The TTF Linac was constructed to gain experience with the new components (cavities, klystrons, diagnostics, etc.) during continuous long term operation. As of writing, the total beam time at the TTFL was about 8,000 h. In addition, important experience with the FEL operation was obtained [39] (see also chapter 9).

2.2.2 Layout of the TTF linac

The TTF linac at DESY has been designed, built, installed and operated by the TESLA collaboration. The schematic of the linac is shown in figure 2.2.1.

The TTFL in its present set-up consists of the following sections:

- injector area;
- two accelerator modules;
- bunch compressor section;
- collimator section;
- undulator; and
- high energy beam analysis area together with the photon beam diagnostics.

The injector area includes the electron gun, the superconducting capture cavity, focusing lenses, and beam diagnostic equipment for the full characterisation of the electron beam properties. The capture cavity is identical to one of the standard nine-cell structures in the main linac. The principal parameters of the injector are listed and discussed in the following sections.

The two installed cryomodules (each 12.2 m in length) comprise the main body of the linac (figure 2.2.2). Each cryomodule contains eight nine-cell cavities, a superconducting quadrupole / steerer package, and a cold cavity type beam position monitor. Each accelerating structure has an input coupler for RF power, a pickup antenna to measure the cavity field amplitude and phase, two HOM damping couplers, and a frequency tuning mechanism. The two cryomodules are connected by a cryogenic line bypassing the bunch compressor.

The bunch compressor section between the two cryomodules is used to reduce the electron bunch length produced in the electron gun by roughly a factor of four. The shortening of the bunch increases the peak bunch current to several hundred amps, which is required for a high gain of the FEL.

A collimator section in front of the undulator protects the vacuum system as well as the permanent magnets of the undulator. Because of the small electron beam diameter in the undulator, a beam loss in this approximately 15 m long section would be a high risk for the linac vacuum system. Radiation from beam losses could also cause a reduction of the magnetisation of the permanent magnet material in the undulator.

The undulator consists of three sections, each 4.5 m in length. The sinusoidal magnetic field has a period of 2.73 cm. Focusing of the beam is accomplished using additional permanent quadrupole magnets. Beam position monitors and wire scanners are installed between each section and in front and behind of the complete undulator. Additional beam position monitors within the undulator sections themselves can be used for improving the needed overlap between the magnetic axis of the undulator, the electron beam, and the emitted photon beam.

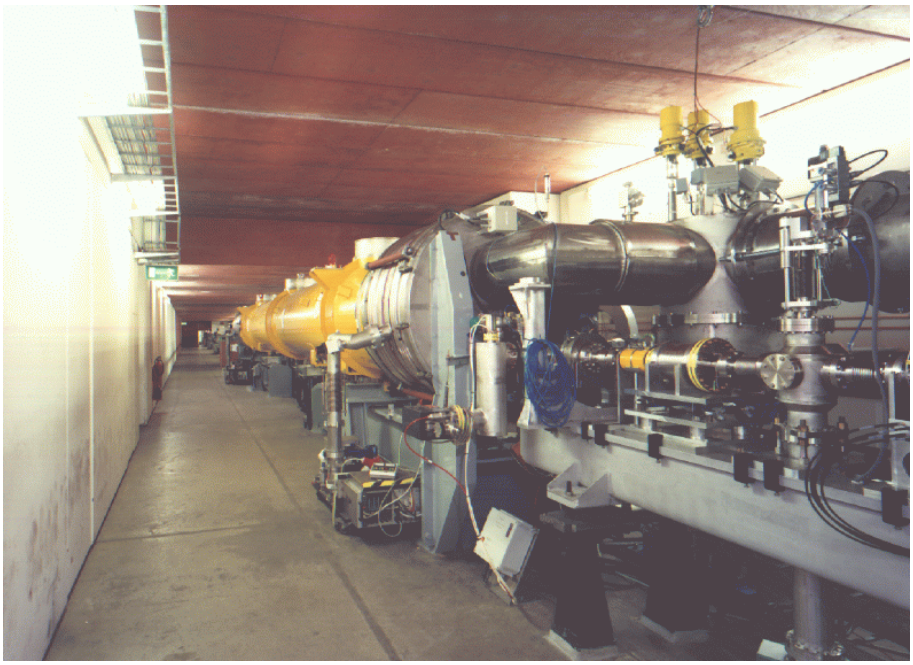

Figure 2.2.2: *View into the TTF Linac tunnel. The electron beam (already accelerated by the capture cavity) comes from the right and is injected into the first accelerator module, which can be seen in the background (yellow vessel).*

The high energy beam analysis area allows the full analysis of the electron beam parameters. Transverse profile, divergence, energy, energy spread, and bunch charge can be measured bunch by bunch. Other measurements (e.g. bunch length) require a scan over several bunches. The photon diagnostic section downstream of the undulator allows the full characterisation (intensity, time structure, and spatial distribution) of the FEL photon beam.

2.2.3 Parameters of the TTF linac

The design parameters for the TTF Linac are summarised in table 2.2.1. The achieved parameters listed summarise the results of the year 2000 run. A description of the various experiments, component development, and achievements is presented in the following sections.

2.2.4 Electron gun

The test of superconducting cavities with the design bunch charge and beam pulse current and length was planned as part of the TTF program. A radio frequency (RF) gun is the state-of-the-art way to generate this electron beam. Furthermore, the X-ray FEL requires bunches of sub-picosecond length at 1 nC charge. At present only laser-driven RF photocathode guns are capable of producing such ultrashort bunches. The

Injector		TTF Linac design/achieved	
		Inj. I	Inj. II
Injector Energy [MeV]		10 / 12	20 / 16
Norm.Emittance [pi mm mrad]			
at 37 pC (only Inj.I)		5 / 3	
at 8 nC (only Inj.II)			20 / 15
at 1 nC (only Inj.II)			2 / 4
Bunch frequency [MHz]		217 / 217	1-9 / 0.1-2.25
Bunch charge [nC]		0.037 / 0.037	1-8 / 0.1-10
Linac	TESLA	TTF Linac designed / achieved	
Linac Energy [MeV]	250000	255 / 300	
RF frequency [GHz]	1.3	1.3	
Accel.Gradient [MV/m] with beam	23.4	15 / 14, 19, 22	
Unloaded quality factor [10^{10}]	1.0	0.3 / > 1.0	
No. of Cryomodules	2628	4 / 3 + 2	
Energy Spread, single bunch rms	5×10^{-4}	$\approx 10^{-3}/10^{-3}$	
Energy variation, bunch to bunch	5×10^{-4}	$\approx 2\times10^{-3}$ / 2×10^{-3}	
Bunch length, rms [μm]	300	1000 / 400	
Beam current [mA]	9.5	8 / 8	
Beam macro pulse length [μs]	950	800 / 800	

Table 2.2.1: *TESLA-500 – TTF Linac parameters comparison.*

small emittance can be preserved by rapidly accelerating the electrons to relativistic energies where the effects of space charge forces become small. For these reasons an RF gun was chosen as the electron source for the TTF linac, although the specified beam macro pulse length of 800 μs presented a considerable challenge.

Since the development of the RF gun required some time, a thermionic gun was used in the first injector (INJ1) [40] of the TTF linac. The grid of the thermionic gun was modulated with a subharmonic of the main RF frequency, $1300/6 = 217$ MHz, to produce an 800 μs long train of electron bunches with a charge of 37 pC, a length of 660 ps and a spacing of 4.6 ns. After electrostatic acceleration to 250 keV the electrons were injected into a 217 MHz copper cavity where a velocity modulation was imposed on the particles to achieve a longitudinal compression in the following drift space. A superconducting 9-cell cavity, the booster cavity in figure 2.2.1, raised the energy to 12 MeV. This electron beam has been used to commission the TTF linac and to check many technical components. In particular it has been possible to operate the superconducting cavities with full beam loading [41] and to verify the proper functioning of the klystron, the high power RF distribution system and the digital RF control system. Furthermore, first studies of higher-order modes and multibunch effects were made using this injector (see below).

The development of an RF gun was started at FNAL, based on the existing design of operating RF guns at BNL and Los Alamos. Later, an alternative design was

pursued at DESY [43] which tried to optimise the gun with respect to the FEL beam emittance requirements: a coaxial RF input coupler was used, which improved the axial symmetry of the accelerating field and gave more freedom to optimize the pattern of the superimposed magnetic field at the cathode (i.e. the position of focusing solenoids).

The main challenges of the RF gun development were:

- the long macro pulse of 800 μs length;
- the high gradient of 35 MV/m at the cathode surface;
- a long life time of Cs_2Te cathodes with high quantum efficiency;
- experience with a cathode preparation system [44].

In addition, the development of a UV laser with sufficiently high power and a pulse structure suitable to produce the required electron beam time structure [45] presented a considerable challenge.

The FNAL RF gun has been in use at DESY since 1998. The laser, RF supply (∼2.2 MW), amplitude and phase controller, water cooling system, and cathode preparation and handling system are all used routinely. At gradients above 30 MV/m we routinely have 800 μs long RF pulses in the gun. The dark current (typically 100 μA) at the gun exit is low enough to scrape off. The laser produces the required pulse structure, although for FEL operation the pulse length should be shortened. Gun conditioning is, however, problematic and generally time consuming, and additional minor design problems are still under investigation. Details of the results of the operation of the FNAL RF gun are given in [46]. Further R&D on the gun and beam transport to the first accelerating module will be carried out using the DESY RF gun [47].

2.2.5 Booster cavity and low energy beam analysis area

The approximately 4 MeV electron beam from the RF gun is injected into the booster cavity which is a standard nine-cell TESLA cavity. This cavity was one of the first prepared for the TTFL. Its field emission onset is about 14 MV/m. A feedback system [48] allows the cavity to operate with an amplitude stability better than 0.1%, and a phase stability of better than 1°. The cavity was operated with full beam loading and with the design beam parameters. The typical beam energy downstream of the capture cavity is 16 MeV.

The beam transport system at 16 MeV consists of a magnetic dipole chicane, a spectrometer section ending at a beam dump, and the straight matching section to the first accelerator module. The chicane was installed to study bunch shortening at low energies. The challenge facing the injector beam transport is to achieve a low emittance as well as a short bunch length under the presence of large space charge forces. At 1 nC the optimized normalized emittance was measured at 4 mm mrad, and at 8 nC approximately 15 mm mrad [49, 50].

The spectrometer arm is used to tune the injector with respect to energy and energy spread. At 16 MeV beam energy the optimized relative energy spread was measured at 0.2 % (rms).

2.2.6 Accelerator modules

The layout of the TTF linac accelerator modules is very similar to the layout for the TESLA main linac, which is described in detail in section 3.3. The main difference is the length, which is about 12 m for the TTF modules and about 17 m for TESLA. The reason is that the TTF modules accommodate eight 9-cell cavities whereas 12 cavities are foreseen for the TESLA linac modules.

Results of measurements of the static heat load at the various temperature points are listed in table 2.2.2. The somewhat higher value at 2 K with respect to the design heat load is due to the cables for additional diagnostics (e.g. temperature sensors, vibration sensors), which will not be present in the TESLA linac modules.

	static load (design)	static load (meas.)
at 2 K / Watts	2.8	4
at 4.5 K / Watts	13.9	13
at 70 K / Watts	76.8	78

Table 2.2.2: *Summary of TTF heat load for one accelerator module.*

As of writing five accelerator modules have been built since the beginning of the TTF programme. Three of them have been installed in the TTFL; the last two are foreseen for the extension of the linac to higher energies. Cavities operated in the TTFL have shown slightly lower gradients compared to the vertical or horizontal cavity tests (see figure 2.1.11 in section 2.1.5.5); this is because of different field emission onsets, and because the operation of several cavities connected to one single klystron is limited by the worst cavity. The maximum gradients achieved (at quality factors higher or equal to the design value of $Q_0 = 10^{10}$) with the three modules are given in table 2.2.3.

In the linac a total of 16 cavities are driven by one klystron. The cavities have been routinely operated at a gradient of ≈15 MV/m providing a 260 MeV beam for different experiments including stable FEL operation. The achieved relative amplitude stability of 2×10^{-3} and absolute phase stability of 0.5° complies with the requirements. Residual fluctuations are dominated by a repetitive component which can be further reduced be using an adaptive feedforward, significantly surpassing the design goals (see section 3.4 and [51]).

module No.	module name	RF test ($Q_0 > 10^{10}$)	beam operation
1	1 (ACC1 old)	17.5	14
2	2 (ACC2)	21.2	19
3	3 (ACC1 new)	23.6	22
4	4	25.4	to be tested
5	1*	25.3	to be tested

Table 2.2.3: *Gradients achieved in the TTF Linac accelerator modules.*

One of the major challenges for the RF control of superconducting cavities is the Lorentz force detuning: the electromagnetic field inside the structures deforms the cavity causing it to detune. The frequency change scales with the square of the accelerating gradient and depends on the mechanical stiffness of the cavities. At high gradients the frequency change is comparable with the bandwidth, and the stabilization of the field amplitude requires additional RF power. Recently an active system was successfully tested which compensates the frequency detuning by means of a piezoelectric tuner (see section 2.1).

The transport of very low emittance beams along the TESLA linac requires transverse higher-order mode (HOM) damping: the HOM Q values should not exceed $\sim 10^5$. HOM couplers mounted on the beam tubes of the TESLA nine-cell superconducting cavities are foreseen for this purpose. So-called 'trapped' modes whose energy is concentrated in the central cells of the cavity can only be detected using the accelerated electron beam [52]. In a dedicated experiment using an intensity-modulated beam from injector-I, a high-order 2585 MHz dipole mode was found with a Q factor up to 9×10^5 [53]. The mode could be identified with the highest mode of the third dipole passband. The high Q factor is outside the specifications for the TESLA linac, but is expected to be avoidable by a better control of the cavity's geometry or a slight re-positioning of the HOM coupler (or both).

One of the measurements performed with long beam pulses is shown in figure 2.2.3. An almost 800 μs long macro pulse comprising 1800 bunches with more than 3 nC bunch charge each was accelerated in the TTF Linac. With the macro pulse current being about 8 mA, the bunch charge was stable within ~10%, the achieved energy stability was σ_E/E=0.07%. The above mentioned RF control of the superconducting cavities was used together with a beam loading compensation.

2.2.7 Bunch Compressor

The free-electron laser operation mode of the TTFL requires short electron bunches with high intensity. Therefore a bunch compressor is inserted between the two accelerating modules to increase the peak current of the bunch up to 500 A, corresponding to 0.25 mm bunch length (rms) for a 1 nC bunch with Gaussian density profile. The compression is achieved by making use of the path length difference for particles of different energy in a bending magnet system (chicane). By accelerating the bunches slightly off-crest in the RF wave, particles in the bunch head have a lower energy than in the tail and thus travel a longer distance in the chicane.

It is routinely verified that a large fraction of the bunch charge is compressed to a length below 0.4 mm (rms) [54]. In addition there are indications that the core is compressed even further, giving an estimated peak current of 400 ± 200 A. At these short bunch lengths, coherent synchrotron radiation produced in the magnetic chicane may affect the emittance and the energy spread of the bunch [55].

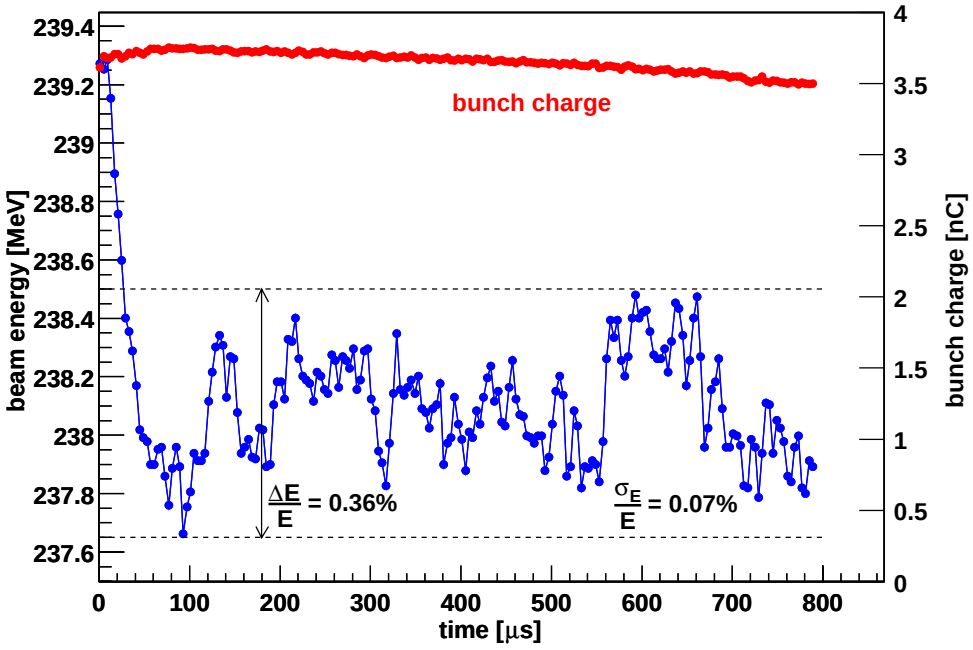

Figure 2.2.3: *Acceleration of long macro pulses. The beam energy and the bunch charge within one single macro pulse are shown. The RF control system was operated with beam loading compensation. The bunch spacing was 444 ns.*

2.2.8 Collimator

The second installed accelerator module of the TTFL is followed by a collimator section which combines the transverse matching of the electron beam to the undulator with the protection of the undulator vacuum chamber and magnets. As a consequence of the small beta function in the undulator — typically 1 m, corresponding to an rms beam sizes of $\sim$100 μm — it only requires 10 bunches with 1 nC charge to burn a hole into the vacuum chamber. In addition radiation damage of the Sm_2Co_{17} permanent magnets in the undulator from either beam halo (dark current) or direct beam loss could degrade the field quality. The collimator consists of a pair of spoiler / absorber units, and the optics (quadrupole settings) is matched so that the physical apertures of the downstream undulator lie within the collimator shadow.

2.2.9 Undulator

The undulator is a 12 mm gap permanent magnet device which uses a combined function magnet design [56]. It has a period length of 27.3 mm and a peak magnetic field of 0.46 T, resulting in an undulator parameter of K = 1.17. The beam pipe diameter in the undulator (9.5 mm) [57] is much larger than the beam diameter (300 μm). Electron beam focusing is achieved by integrated quadrupoles producing a gradient of 12 T/m superimposed on the periodic undulator field. The undulator system is subdivided

into three segments, each 4.5 m long and containing 10 quadrupole sections, i.e. 5 full focusing-defocusing (FODO) cells. The FODO lattice periodicity runs smoothly from segment to segment. There is a spacing of 0.3 m between adjacent undulator segments for diagnostics (e.g. wire scanners [58]). The total length of the undulator section is 14.1 m. The vacuum chamber incorporates beam position monitors and orbit correction magnets (one for each quadrupole).

The first observation of SASE in a free-electron laser was at the beginning of year 2000 (see section 9.2 and [39]). The emitted radiation was in the Vacuum Ultraviolet range between 80 nm and 180 nm wavelength. Later in the year, the SASE gain was increased to approximately 10^5. For the radiation intensity measurements different detectors were used [59].

2.2.10 Beam diagnostics

The high energy beam analysis area at the end of the TTFL allows the full analysis of the electron beam parameters. Transverse profile and beam divergence are measured using optical transition radiation (OTR) screens [60] as well as diffraction radiators [61]. Energy and energy spread are measured in the dispersive section again using OTR screens. A system combining the readout of different toroid monitors installed in all sections (from the gun to the beam dump) measures the beam intensity and monitors the transmission along the linac; together with a number of photo-multipliers, it forms part of the interlock system and protects the TTFL against excessive beam losses.

The above measurements can be made on a single bunch: measurement of the bunch length requires averaging over several bunches. A bunch length monitor using interferometry of coherent transition radiation is located downstream of the second accelerator module.

The symbiosis between the accelerator module test and FEL operation has proven useful with respect to the development of new diagnostic techniques. The measurement of wakefields excited by bunches of different length [62] and the test of a beam trajectory monitor for the TTF FEL undulator [63] are two good examples.

Bibliography

[1] Proceedings of the 1st TESLA WORKSHOP, CLNS-90-1029, edited by H. Padamsee, Cornell University, USA, 1990.

[2] C. Reece et al., *Performance Experience with the CEBAF SRF Cavities*, Proc. Particle Accelerator Conference and International Conference on High Energy Accelerators, Dallas 1995, p. 1512.

[3] G. Müller, Proc. 3^{rd} Workshop on RF Superconductivity, ANL-PHY-88-1, Argonne, USA, 1988, edited by K.W. Shepard, p. 331.

[4] A. Boucheffa et al., Proc. 7^{th} Workshop on RF Superconductivity, CEA/Saclay 96 080/1, Gif-sur-Yvette, France, 1995, edited by B. Bonin, p. 659.

[5] H. Padamsee, J. Knobloch and T. Hays, *RF Superconductivity for Accelerators*, John Wiley, New York, 1998.

[6] P. Kneisel, Proceedings of the Workshop on RF Superconductivity, KFK 3019, Karlsruhe, Germany, 1980, p. 27.

[7] Ph. Bernard et al., *Superconducting Niobium Sputter-Coated Copper Cavities at 1500 MHz*, Proc. 3^{rd} EPAC, Berlin 1992, p. 1269.

[8] C. Crawford et al., *High Gradients in Linear Collider Superconducting Accelerator Cavities by High Pulsed Power to Suppress Field Emission*, Particle Accelerators **49** (1995) 1.

[9] M. Liepe, *Pulsed Superconductivity Acceleration*, Proc. 20^{th} International Linac Conference, Monterey 2000, to be published.

[10] K. Saito et al., Proc. 4th Workshop on RF Superconductivity, KEK Report 89-21, p. 635, Tsukuba, Japan, 1989.

[11] L. Ponto and M. Hein, External Report from Bergische Universität Wuppertal, WUB 86-17, Wuppertal, Germany, 1986.

[12] K. Saito et al., Proc. 8^{th} Workshop on RF Superconductivity, Abano Terme, Italy 1997, edited by V. Palmieri and A. Lombardi, published in Particle Accelerators **60** (1998) 193.

[13] E. Kako et al., *Improvement of Cavity Performance in the Saclay/Cornell/DESY's SC Cavities*, Proc. 9^{th} Workshop on RF Superconductivity, Santa Fe, USA, 1999 (to be published).

[14] L. Lilje et al., *Electropolishing and in-situ Baking of 1.3 GHz Niobium Cavities*, Proc. 9^{th} Workshop on RF Superconductivity, Santa Fe, USA, 1999 (to be published).

[15] B. Visentin et al., *Cavity Baking: A Cure for the High Accelerator Field Q_0 Drop*, Proc. 9^{th} Workshop on RF Superconductivity, Santa Fe, USA, 1999 (to be published).

[16] S. Bousson, *Advances in Superconducting RF Cavity Stiffening by Thermal Spraying*, Proc. 9^{th} Workshop on RF Superconductivity, Santa Fe, USA, 1999 (to be published).

[17] M. Liepe, W.D. Moeller, S.N. Simrock, *Dynamic Lorentz Force Compensation with a Fast Piezoelectric Tuner*, DESY TESLA-01-03, 2001.

[18] V. Palmieri, in Proc. 8^{th} Workshop on RF Superconductivity, Abano Terme, Italy, 1997, edited by V. Palmieri and A. Lombardi, p. 553 and LNL-INFN (Rep) 133/98.

[19] V. Palmieri et al., *Spun TESLA-type Cavities: Results from a Worldwide Collaboration*, LNL INFN (REP) 176/2001.

[20] P. Kneisel, V. Palmieri and K. Saito, *Development of Seamless Niobium Cavities for Accelerator Application*, Proc. 9^{th} Workshop on RF Superconductivity, Santa Fe, USA, 1999 (to be published).

[21] W. Singer, I. Gonin, I. Jelezov, H. Kaiser, T. Khabibuline, P. Kneisel, K. Saito, X. Singer, *Hydro Forming of TESLA Cavities at DESY*, Proc. 7^{th} EPAC, Vienna 2000.

[22] C. Benvenuti et al., *High-Q, High Gradient Niobium-Coated Cavities at CERN*, Proc. 9^{th} Workshop on RF Superconductivity, Santa Fe, USA, 1999 (to be published).

[23] P. Bosland, A. Aspart, E. Jacques and M. Ribeaudeau, IEEE Transactions on Applied Superconductivity, ASC'98, Vol. 9, 896 (1999).

[24] M. Champion et al., TESLA Input Coupler Development, Proc. Particle Accelerator Conf., Washington 1993, Vol. II, p. 809.

[25] S. Chel et al., *Power Coupler Development for SC Cavities*, Proc. 5^{th} EPAC, Sitges 1996, p. 2088.

[26] S. Chel et al., *Status of the TESLA Power Coupler Development Programme in France*, Proc. 6^{th} EPAC, Stockholm 1998, p. 1882.

[27] S. Chel et al., *Coaxial Disc Windows for a High Power Superconducting Cavity Input Coupler*, Proc. 18^{th} Particle Accelerator Conf., New York 1999, p. 916.

[28] W. D. Möller, *High Power Coupler for the TESLA Test Facility*, Proc. 9^{th} Workshop on RF Superconductivity, Santa Fe, USA, 1999 (to be published).

[29] M. Ukkola and P. Ylä-Oijala, *Numerical Simulation of Electron Multipacting in TTF III Cold Window with a DC Bias*, Helsinki Institute of Physics, Finland, Technical Report, 2000.

[30] S. Michizono, A. Kinbara et al., *TiN Film Coatings on Alumina Radio Frequency Windows*, J. Vac. Sci. Technol. **A 10** (4) 1992.

[31] J. Tückmantel et al., *Improvements to Power Couplers for the LEP2 Superconducting Cavities*, Proc. Particle Accelerator Conference and International Conference on High Energy Accelerators, Dallas 1995, Vol III, p. 1642.

[32] J. Sekutowicz, M. Ferrario, C. Tang, *Superconducting superstructure for the TESLA collider: A concept*, Phys. Rev. ST Accelerators and Beams 2:062001, 1999.

[33] M. Ferrario, A. Mosnier, L. Serafini, F. Tazzioli, J.M. Tessier, *Multi-Bunch Energy Spread Induced by Beam Loading in a Standing Wave Structure*, Particle Accelerators **52** (1996) 115.

[34] M. Dohlus, H. W. Glock, D. Hecht and U. van Rienen, *Filling and Beam Loading in TESLA Superstructures*, DESY TESLA-98-14, 1999.

[35] N. Baboi, R. Brinkmann, M. Liepe and J. Sekutowicz, *HOM Damping Requirements for the TESLA Superstructures*, Proc. 7^{th} EPAC, Vienna 2000, p. 2016.

[36] *Proposal for a TESLA Test Facility*, DESY TESLA-93-01, 1992.

[37] TESLA Collaboration, ed. D.A. Edwards, *TESLA Test Facility Linac - Design Report*, DESY TESLA-95-01, 1995.

[38] *A VUV Free Electron Laser at the TESLA Test Facility - Conceptual Design Report*, DESY TESLA-FEL-95-03, 1995.

[39] J. Andruszkow et al., *First Observation of Self-Amplified Spontaneous Emission in a Free-Electron Laser at 109 nm Wavelength*, Phys. Rev. Lett. **85** (2000) 3825.

[40] B. Aune, M. Jablonka, J. M. Joly and E. Klein, *A Low Charge per Bunch Injection Line for the TESLA Test Facility*, DESY TESLA-93-04, 1993.

[41] T. Garvey et al., *First Beam Tests of the TTF Injector*, Proc. Particle Accelerator Conference, Vancouver 1997, p.2823.

[42] E. Colby, *Experimental Testing of the TTF RF Photoinjector*, Proc. Particle Accelerator Conference, Vancouver 1997, p.2873.

[43] B. Dwersteg et al., *RF Gun Design for the TESLA VUV Free Electron Laser*, Proc. 18^{th} International FEL Conference, Rome 1996, p.93.

[44] P. Michelato et al., *Cs_2Te Photocathode for the TTF Injector II*, Proc. 5^{th} EPAC, Sitges 1996, p.1510.

[45] S. Schreiber et al., *Running Experience with the Laser System for the RF Gun Based Injector at the TESLA Test Facility Linac*, Nucl.Instr. and Methods **A445** (2000) 427.

[46] S. Schreiber for the TESLA Coll., *First Experiments with the RF Gun Based Injector for the TESLA Test Facility Linac*, Proc. Particle Accelerator Conference, New York 1999, p. 84.

[47] F. Stephan et al., *Photo Injector Test Facility under Construction at DESY Zeuthen*, FEL'2000 Conference, submitted to NIM.

[48] A. Mosnier et al., *RF Control System for the SC Cavity of the TESLA Test Facility Injector*, Proc. Particle Accelerator Conference, Vancouver 1997, p.2311.

[49] Ph. Piot et al., *Transverse Phase Space Studies in TTF Photoinjector During Run 00-01: A Comparison between Simulation and Experiment*, DESY TESLA-FEL-00-04, 2000.

[50] M. Geitz et al., *Phase Space Tomography at the TESLA Test Facility Linac*, Proc. Particle Accelerator Conference, New York 1999, p.2175.

[51] S.N. Simrock et al., *Design of the Digital RF Control System for the TESLA Test Facility*, Proc. 5^{th} EPAC, Sitges 1996, p. 349.

[52] S. Fartoukh, *A New Method to Detect the High Impedance Dipole Modes of TESLA Cavities*, DESY TESLA-98-13, 1998.

[53] S. Fartoukh et al., *Evidence For a Strongly Coupled Dipole Mode with Insufficient Damping in TTF First Accelerating Module*, Proc. Particle Accelerator Conference, New York 1999, p. 922.

[54] M. Geitz et al., *Sub-Picosecond Bunch Length Measurement at the TESLA Test Facility*, Nucl. Instr. and Methods **A445** (2000) 343.

[55] M. Dohlus et al., *Optimal Beam Optics in the TTF-FEL Bunch Compression Section: Minimizing the Emittance Growth*, Proc. Particle Accelerator Conference, New York 1999, p. 1650.

[56] Y.M. Nikitina, J. Pflüger, *Two Novel Undulator Schemes With Quadrupolar Focusing for the VUV-FEL at the TESLA Test Facility*, Nucl. Instr. and Methods **A375** (1996) 325.

[57] U. Hahn et al., *Design and Performance of the Vacuum Chambers for the Undulator of the VUV FEL at the TESLA Test Facility at DESY*, Nucl. Instr. and Methods **A445** (2000) 442.

[58] G. Schmidt et al., *First Results of the High Resolution Wire Scanners for Beam Profile and Absolute Beam Position Measurement at the TTF*, FEL'2000 Conference, submitted to NIM.

[59] Ch. Gerth et al., *Photon Diagnostics for the Study of Electron Beam Properties of a VUV SASE FEL at DESY*, FEL'2000 Conference, submitted to NIM.

[60] M. Castellano et al., *Time Resolved Energy Measurement of the TESLA Test Facility Beam Through the Analysis of Optical Transition Radiation Angular Distribution*, Proc. Particle Accelerator Conference, New York 1999, p. 2196.

[61] M. Castellano et al., *Bunch Length Measurements at TTF Using Coherent Diffraction Radiation*, Proc. 7^{th} EPAC, Vienna 2000, p. 1699.

[62] M. Huening et al., *Experimental Setup to Measure the Wake Fields Excited by a Rough Surface*, Nucl.Instr. and Methods **A445** (2000) 362.

[63] S. Hillert et al., *The Beam trajectory Monitor for the TTF-FEL at DESY*, Proc. 7^{th} EPAC, Vienna 2000, p 1803.